ORIGINAL RESEARCH

# Nitric Oxide–Dependent Feedback Loop Regulates Transient Receptor Potential Vanilloid 4 (TRPV4) Channel Cooperativity and Endothelial Function in Small Pulmonary Arteries

Corina Marziano, MS;* Kwangseok Hong, PhD;* Eric L. Cope, BS; Michael I. Kotlikoff, VMD, PhD; Brant E. Isakson, PhD; Swapnil K. Sonkusare, PhD

***Background***—Recent studies demonstrate that spatially restricted, local $Ca^{2+}$ signals are key regulators of endothelium-dependent vasodilation in systemic circulation. There are drastic functional differences between pulmonary arteries (PAs) and systemic arteries, but the local $Ca^{2+}$ signals that control endothelium-dependent vasodilation of PAs are not known. Localized, unitary $Ca^{2+}$ influx events through transient receptor potential vanilloid 4 (TRPV4) channels, termed TRPV4 sparklets, regulate endothelium-dependent vasodilation in resistance-sized mesenteric arteries via activation of $Ca^{2+}$-dependent $K^+$ channels. The objective of this study was to determine the unique functional roles, signaling targets, and endogenous regulators of TRPV4 sparklets in resistance-sized PAs.

***Methods and Results***—Using confocal imaging, custom image analysis, and pressure myography in fourth-order PAs in conjunction with knockout mouse models, we report a novel $Ca^{2+}$ signaling mechanism that regulates endothelium-dependent vasodilation in resistance-sized PAs. TRPV4 sparklets exhibit distinct spatial localization in PAs when compared with mesenteric arteries, and preferentially activate endothelial nitric oxide synthase (eNOS). Nitric oxide released by TRPV4-endothelial nitric oxide synthase signaling not only promotes vasodilation, but also initiates a guanylyl cyclase-protein kinase G-dependent negative feedback loop that inhibits cooperative openings of TRPV4 channels, thus limiting sparklet activity. Moreover, we discovered that adenosine triphosphate dilates PAs through a P2 purinergic receptor-dependent activation of TRPV4 sparklets.

***Conclusions***—Our results reveal a spatially distinct TRPV4-endothelial nitric oxide synthase signaling mechanism and its novel endogenous regulators in resistance-sized PAs. **(*J Am Heart Assoc*. 2017;6:e007157. DOI: 10.1161/JAHA.117.007157.)**

**Key Words:** calcium channel • calcium signaling • endothelial nitric oxide synthase • endothelium • microcirculation • pulmonary artery • signaling pathways • transient receptor potential vanilloid 4 channel • vascular endothelial function



Endothelial cells (ECs) from small, resistance-sized arteries are key controllers of vascular resistance. Recent studies in systemic arteries—including mesenteric, cremaster, and cerebral arteries—have demonstrated that endothelium-dependent vasodilation is controlled by local, spatially restricted increases in endothelial $Ca^{2+}$ while the whole-cell $Ca^{2+}$ level remains unchanged.[1–5] In contrast to systemic arteries, pulmonary arteries (PAs) comprise a low-pressure, high-flow circulation. Moreover, systemic and pulmonary vascular resistances can be regulated independently.[6] The distinct signaling mechanisms that regulate endothelial function in small PAs are poorly understood. Unraveling the local $Ca^{2+}$ signals in small PAs may be necessary for understanding endothelial regulation of pulmonary vascular resistance under normal and disease conditions.

In mesenteric, cremaster, and cerebral arteries, transient receptor potential vanilloid 4 (TRPV4) channels are key regulators of endothelium-dependent vasodilation.[1,4,7] In mesenteric arteries, local, unitary $Ca^{2+}$ influx events through endothelial TRPV4 channels, termed "TRPV4 sparklets," activated endothelial IK/SK ($Ca^{2+}$-activated intermediate and small conductance $K^+$) channels to cause vasodilation.[4,5] The biophysical properties, signaling targets, and endogenous regulators of TRPV4 sparklets in small PAs remain

*From the Departments of Molecular Physiology and Biological Physics (C.M., B.E.I., S.K.S.) and Pharmacology (S.K.S.), and Robert M. Berne Cardiovascular Research Center (C.M., K.H., E.L.C., B.E.I., S.K.S.), University of Virginia School of Medicine, Charlottesville, VA; Department of Biomedical Sciences, College of Veterinary Medicine, Cornell University, Ithaca, NY (M.I.K.).*

Accompanying Figures S1 through S6 and Video S1 are available at http://jaha.ahajournals.org/content/6/12/e007157.full#sec-32

*Ms Marziano and Dr Hong are co-first authors.

**Correspondence to:** Swapnil K. Sonkusare, PhD, Robert M. Berne Cardiovascular Research Center, University of Virginia School of Medicine, MR4 Room 6051A, 409 Lane Rd, Charlottesville, VA 22901. E-mail: sks2n@virginia.edu

Received September 6, 2017; accepted November 1, 2017.

## Clinical Perspective

### What Is New?

- Our studies reveal a novel transient receptor potential vanilloid (TRPV4) channel-dependent $Ca^{2+}$ signaling mechanism that regulates endothelial function in small pulmonary arteries.
- Unitary $Ca^{2+}$ influx signals through TRPV4 channels (TRPV4 sparklets) activate endothelial nitric oxide synthase in small pulmonary arteries. NO released by TRPV4- endothelial nitric oxide synthase signaling initiates guanylyl cyclase (GC)-protein kinase G (PKG) signaling in the endothelium that limits TRPV4 channel cooperativity and serves as a negative feedback signal to regulate TRPV4 channel function.
- Furthermore, ATP dilates small pulmonary arteries predominantly via activation of TRPV4-endothelial nitric oxide synthase signaling.

### What Are the Clinical Implications?

- Abnormalities in TRPV4-dependent endothelial $Ca^{2+}$ signaling may be a potential pathological mechanism that contributes to endothelial dysfunction in pulmonary vascular disorders.
- Individual elements in the TRPV4-dependent endothelial $Ca^{2+}$ signaling pathway may offer novel therapeutic targets for treating pulmonary hypertension and other pulmonary vascular disorders.

unknown. Endothelium-derived nitric oxide (NO) is thought to be the predominant vasodilator in the pulmonary circulation.[8–12] Increase in global $Ca^{2+}$ has long been associated with activation of endothelial nitric oxide synthase (eNOS). Whether a specific local $Ca^{2+}$ signal can activate eNOS has not been elucidated. In this study, we explored the possibility that local, unitary $Ca^{2+}$ influx through TRPV4 channels activates eNOS in small PAs, a signaling mechanism different from small mesenteric/cremaster/cerebral arteries.[1,4,7]

NO can alter the activity of several ion channels by *S*-nitrosylation or activation of guanylyl cyclase-protein kinase G (GC-PKG) signaling.[13–17] In cultured cells, *S*-nitrosylation of TRPV4 channels increased the channel function,[18] and activation of GC-PKG signaling reduced the channel activity.[19] Therefore in PAs, TRPV4-eNOS signaling could activate a bidirectional regulation, where TRPV4 channels promote NO release, which in turn regulates TRPV4 channel function. $Ca^{2+}$-dependent cooperative opening of TRPV4 channels in a cluster has emerged as a key mechanism for modulating TRPV4 channel function.[4,5,20,21] We postulated that TRPV4-induced NO release modulates TRPV4 channel activity by altering cooperative openings of TRPV4 channels.

Discovering the endogenous activators of TRPV4 channels in small PAs is central to deciphering the unique physiological roles of TRPV4 channels in pulmonary circulation. In this regard, purinergic receptor agonist ATP has been shown to increase endothelial $Ca^{2+}$ and cause vasodilation in large, conduit PAs.[22–24] ATP can be released into the circulation by ECs, smooth muscle cells (SMCs), and red blood cells.[25,26] Circulatory ATP may, therefore, serve as an important regulator of pulmonary vascular resistance. We hypothesized that ATP is a novel, endogenous activator of TRPV4 channels in small PAs.

In the current study we provide the first evidence that local $Ca^{2+}$ signals–TRPV4 sparklets–regulate baseline and induced eNOS activity to dilate small PAs. Moreover, we report ATP as a novel endogenous activator of TRPV4 channels that promotes TRPV4-eNOS signaling through P2 purinergic receptors. NO is another endogenous regulator of TRPV4 channels that limits TRPV4 channel activity by disrupting the coupling among TRPV4 channels via activation of endothelial GC-PKG mechanism. These results reveal distinct, novel local $Ca^{2+}$ signaling mechanisms that regulate endothelial function in small PAs.

## Methods

The data that support the findings of this study are available from the corresponding author upon reasonable request.

### Drugs and Chemical Compounds

Apamin, cyclopiazonic acid (CPA), GSK2193874, GSK1016790A, HC067047, NS309, 1400W, *N*ω-propyl-L-arginine hydrochloride, ODQ, RN1747, Rp-8-Br-PET-cGMPS, Suramin, and Tram 34 were purchased from Tocris Bioscience (Minneapolis, MN). ATP and $N^{\omega}$-nitro-L-arginine were obtained from Sigma-Aldrich (St. Louis, MO). DAF-FM diacetate, Fluo-4AM ($Ca^{2+}$ indicator), and EGTA-AM ($Ca^{2+}$ chelator) were purchased from Fischer Scientific (Pittsburgh, PA). Spermine NONOate and U46619 were purchased from Cayman Chemical (Ann Arbor, MI). All other chemicals were obtained from Sigma-Aldrich (St. Louis, MO).

### Animal Procedures

All animal protocols were approved by the Animal Care and Use Committee of the University of Virginia. Male C57BL6/J, transgenic $GCaMP2^{Cx40}$, $TRPV4^{-/-}$, and $eNOS^{-/-}$ (The Jackson Laboratory, Bar Harbor, ME) mice (10–14 weeks old) were used for all the studies. $GCaMP2^{Cx40}$ mice express GCaMP2, a $Ca^{2+}$-specific biosensor under the connexin 40 promoter, thereby limiting its expression to only ECs.[27,28] Mice were euthanized with pentobarbital (90 mg/kg; intraperitoneal) followed by decapitation. Third-order mesenteric arteries

(MAs; ≈100 μm in diameter), fourth-order pulmonary arteries (PAs, ≈100–200 μm), and second-order PAs (≈400 μm) were isolated in cold HEPES-buffered physiological salt solution (HEPES-physiological salt solution [PSS], in mmol/L, 10 HEPES, 134 NaCl, 6 KCl, 1 $MgCl_2$ hexahydrate, 2 $CaCl_2$ dihydrate, and 7 dextrose, pH adjusted to 7.4 using 1 mol/L NaOH). Data were collected from at least 3 different arteries from at least 3 mice.

## Pressure Myography

Isolated PAs and MAs were cannulated on glass pipettes mounted on an arteriography chamber (The Instrumentation and Model Facility, University of Vermont, Burlington, VT) at areas lacking branching points and pressurized to physiological pressure (15 mm Hg for PA and 80 mm Hg for MA). Arteries were superfused with PSS (in mmol/L, 119 NaCl, 4.7 KCl, 1.2 $KH_2PO_4$, 1.2 $MgCl_2$ hexahydrate, 2.5 $CaCl_2$ dihydrate, 7 dextrose, and 24 $NaHCO_3$) at 37°C and bubbled with 20% $O_2$/5% $CO_2$ to maintain the pH at 7.4. All drug treatments were added to the superfusing PSS. Because PAs do not develop myogenic tone at 15 mm Hg, they were preconstricted with 100 nmol/L U46619 (a thromboxane A2 agonist). In functional studies with PAs, all other pharmacological treatments were performed in the presence of U46619. Before measurement of vascular reactivity, arteries were treated with NS309 (1 μmol/L), a direct opener of endothelial IK/SK channel, to assess endothelial health. Arteries that failed to dilate to NS309 were discarded. Endothelial denudation was performed by passing an air bubble through the artery for ≈60 s. Complete removal of the endothelial layer was verified by the absence of dilation to NS309. Changes in arterial diameter were recorded at a 60-ms frame rate using a charge-coupled device camera and edge-detection software (IonOptix LLC, Westwood, MA).[4,5] All drug treatments were incubated for 10 minutes. At the end of each experiment, $Ca^{2+}$-free PSS (in mmol/L, 119 NaCl, 4.7 KCl, 1.2 $KH_2PO_4$, 1.2 $MgCl_2$ hexahydrate, 7 dextrose, 24 $NaHCO_3$, and 5 EGTA) was applied to assess the maximum passive diameter. Percent constriction was calculated by:

$$[(\text{Diameter}_{\text{before}} - \text{Diameter}_{\text{after}})/\text{Diameter}_{\text{before}}] \times 100 \quad (1)$$

where $\text{Diameter}_{\text{before}}$ is the diameter of the artery before a treatment and $\text{Diameter}_{\text{after}}$ is the diameter after the treatment. Percent dilation was calculated by:

$$[(\text{Diameter}_{\text{dilated}} - \text{Diameter}_{\text{basal}})/(\text{Diameter}_{\text{Ca-free}} - \text{Diameter}_{\text{basal}})] \times 100 \quad (2)$$

where $\text{Diameter}_{\text{basal}}$ is the stable diameter before drug treatment, $\text{Diameter}_{\text{dilated}}$ is the diameter after drug treatment, and $\text{Diameter}_{\text{Ca-free}}$ is the maximum passive diameter.

## NO Imaging

PAs and MAs were surgically opened and pinned down on a Sylgard block in en face preparation for NO imaging from intact EC and SMC layers. NO levels were assessed using 5 μmol/L DAF-FM (4-amino-5 methylamino-2′,7′-difluorofluorescenin diacetate) prepared in HEPES PSS with 0.02% pluronic acid.[29] DAF-FM forms a fluorescent triazole compound after binding to NO. En face PAs or MAs were pretreated with GSK101, L-$N^G$-nitroarginine (L-NNA), or GSK219 in HEPES-PSS for 5 minutes at 30°C. Arteries were then incubated with DAF-FM containing the drug under consideration for 20 minutes at 30°C in the dark. Validity of DAF-FM as an NO indicator was tested by treating PAs with NO donor Spermine NONOate (NONOate, 3–30 μmol/L), and recording the DAF-FM fluorescence. Spermine NONOate was selected because it has a long half-life (≈39 minutes) and releases a controlled amount of NO in solution. The experiments using NONOate were performed in the presence of L-NNA to eliminate the effect of endogenous release of NO in response to TRPV4 channel activation. The arteries were incubated with either HEPES-PSS (baseline) or 30 nmol/L GSK101 in the absence or presence of 200 μmol/L L-NNA to determine whether localized $Ca^{2+}$ influx through EC TRPV4 channels contributes to NO release through NOS activation. DAF-FM fluorescence was imaged using Andor Revolution WD (with Borealis) spinning-disk confocal imaging system (Andor Technology, Belfast, UK) comprising an upright Nikon microscope with a ×60 water-dipping objective (numerical aperture 1.0) and an electron-multiplying CCD camera. DAF-FM fluorescence was recorded using an excitation wavelength of 488 nm and emitted fluorescence was captured with a 525/36-nm band-pass filter. Images were obtained along the *z*-axis at a slice size of 0.05 μm from the top of the ECs to the bottom of the SMCs. DAF-FM fluorescence was analyzed using custom-designed SparkAn software by Dr Adrian D. Bonev (University of Vermont, Burlington, VT). An outline was drawn around each EC or SMC to obtain the arbitrary fluorescence intensity of that cell. The background fluorescence was then subtracted from the recorded fluorescence. The fluorescence numbers from all the cells in a field of view were averaged to obtain single fluorescence number for that field. Relative changes in DAF-FM fluorescence were obtained by dividing the fluorescence in the treatment group by that in the control group. Each field of view was considered as n=1, and several fields of view from at least 3 arteries from at least 3 mice were included in the final analysis.

## $Ca^{2+}$ Imaging

Measurement of $Ca^{2+}$ events in the native ECs from PAs was performed as previously described.[4,5] Briefly, Andor

Revolution WD (with Borealis) spinning-disk confocal imaging system described above was used to record $Ca^{2+}$ influx events in en face PAs. $Ca^{2+}$ events were recorded at 30 ms per image before and after 5 minutes of each treatment. The arteries were loaded with fluo-4 AM (10 μmol/L) in the presence of pluronic acid (0.04%) at 30°C for 30 minutes for PAs and 45 minutes for MAs. The majority of experiments were carried out in the presence of CPA (20 μmol/L, a sarcoendoplasmic reticulum (ER) $Ca^{2+}$-ATPase inhibitor) in order to eliminate the interference from $Ca^{2+}$ release from intracellular stores. $Ca^{2+}$ binding-induced changes in emitted fluorescence were observed by exciting at 488 nm with a solid-state laser and collecting emitted fluorescence using a 525/36-nm band-pass filter. In the studies examining whether *S*-nitrosylation of TRPV4 channels mediated the effect of NO on channel activity, flash photolysis using ultraviolet light pulse of 10 ms (Andor Mosaic 3 Infinity, Andor Technology, and pE-4000, CoolLED Ltd, Andover, UK) was conducted to dissociate the S-NO bonds on TRPV4 channels. The experiments using NONOate were performed in the presence of L-NNA to eliminate the effect of endogenous release of NO in response to TRPV4 channel activation. TRPV4 $Ca^{2+}$ sparklets and $Ca^{2+}$ release events from the ER in ECs were analyzed using custom-designed SparkAn software. To generate fractional fluorescence ($F/F_0$) traces, a region of interest defined by a 1.7-$\mu m^2$ (5×5 pixels) box was placed at a point corresponding to peak sparklet amplitude. Each field of view was ≈110×110 μm and covered ≈15 ECs. Representative $F/F_0$ traces were filtered using a Gaussian filter and a cutoff corner frequency of 4 Hz. Sparklet activity, all-points histograms, and coupling coefficients were determined as described previously using the custom-designed SparkAn software, Clampfit, and OriginPro7.5.[4,5]

## Localization of Sparklets at Myoendothelial Projections

To determine the localization of sparklets at myoendothelial projections (MEPs), the arteries were incubated with 100 μmol/L Alexa Fluor 633 hydrazide. Alexa 633 hydrazide cannot penetrate into the cells, but preferentially binds to elastin-containing internal elastic lamina (IEL), thereby illuminating the IEL[1,30] for 15 minutes following $Ca^{2+}$ imaging experiment. The images were then acquired in the fields of view from which $Ca^{2+}$ signals were recorded, using excitation wavelengths of 640 nm (for IEL staining) and 488 nm (for fluo-4), and capturing the emitted fluorescence using 685/40- and 525/36-nm band-pass filters, respectively. Regions of interest (1.7 $\mu m^2$) corresponding to the peak sparklet fluorescence were overlaid onto the IEL staining image. The regions of interest within 5 μm from the center of the holes in the IEL were counted as MEP sparklet sites and the remaining regions of interest were counted as non-MEP sparklet sites, as we have done previously.[5] A sparklet site displays spread of calcium away from the site of initiation. In 88% of sparklet sites, the site of sparklet initiation coincided with the peak sparklet amplitude. Therefore, the region of interest corresponding to the peak sparklet amplitude was used to analyze the sparklet localization data.

## Calculation of Sparklet Activity Per Site and Sparklet Activity Per Field

Activity of TRPV4 $Ca^{2+}$ sparklets was evaluated as described previously.[4,5] Area under the curve for all the events at a site was determined using trapezoidal numerical integration ($[F-F_0]/F_0$ over time, in seconds). The average number of active TRPV4 channels, as defined by $NP_O$ ($NP_O$, where N is the number of channels at a site and $P_O$ is the open state probability of the channel), was calculated by

$$NP_O = (T_{level1} + 2T_{level2} + 3T_{level3} + 4T_{level4})/T_{total} \quad (3)$$

where T is the dwell time at each quantal level detected at TRPV4 sparklet sites and $T_{total}$ is the duration of the recording. $NP_O$ was determined using Single Channel Search module of Clampfit and quantal amplitudes derived from all-points histograms ($\Delta F/F_0$ of 0.29 for Fluo-4–loaded PAs). $NP_O$ for all the sites in a field was averaged to obtain $NP_O$ per site. For the studies on baseline sparklet activity (without GSK101), some of the fields showed no sparklet activity at the baseline but L-NNA still increased the sparklet activity. Therefore, we used $NP_O$ per field instead of $NP_O$ per site to estimate the effect of L-NNA on baseline sparklet activity. All $NP_O$ per site values for all the sites in a field were summated to calculate $NP_O$ per field.

## Construction of All-Points Histograms

As described previously,[4] all-points amplitude histograms were constructed by first filtering $Ca^{2+}$ images with a Kalman filter (adopted from an ImageJ plug-in written by Christopher Philip Mauer, Northwestern University, Chicago, IL; acquisition noise variance estimate=0.05; filter gain=0.8) to assess quantal amplitudes of $Ca^{2+}$ influx events (ie, equal increments of fluorescence signals over increasing numbers of TRPV4 channels). All sparklet events with at least 5 steady baseline points and a steady peak of at least 5 data points were used for the construction of all-points histograms, whereas channel openings with either unstable baseline or shorter duration of opening (eg, fewer than 5 data points at the peak) were excluded from this analysis. The analysis was undertaken with $Ca^{2+}$ images obtained from 3 to 5 fields from 3 to 5 PAs from C57BL6/J or GCaMP2 mice. $F/F_0$ traces were exported to

ClampFit10.3 for constructing all-points histograms, which were then fit with multiple Gaussian function:

$$f(F/F_0) = \sum_{i=1}^{N} \frac{a_i}{\sqrt{2\pi}\sigma_i} \exp\left[\frac{-\left(\frac{F}{F_0} - \mu_i\right)^2}{2\sigma_i^2}\right] \quad (4)$$

where $F/F_0$, a, $\mu$, and $\sigma^2$ represent the fractional fluorescence, area, mean value, and variance of the Gaussian distribution, respectively. Statistical differences in the quantal levels of TRPV4-mediated $Ca^{2+}$ sparklets between diverse treatment regimens were evaluated based on a 95% confidence interval calculated from the mean and SE for each peak.

## Determination of Coupling Coefficients

Coupling coefficients for the coupling among TRPV4 channels at a cluster were determined using a coupled Markov chain model in MATLAB, as previously described.[5,31–34] $[F\text{-}F_0]/F_0$ traces showing steady baseline (ie, at least 30 s duration) were selected for analyzing the cooperative gating of TRPV4 channels. Each TRPV4 sparklet site was examined separately. The coupled Markov chain model developed by Chung and Kennedy[32] was used to simulate and fit independent records of partially coupled channels. Openings of single TRPV4 channel were identified using a single channel amplitude (ie, quantal level) of 0.29 $\Delta F/F_0$ for mouse PAs loaded with fluo-4 and a half-amplitude protocol in a program written in MATLAB. TRPV4 channel activity was considered as a first-order and discrete Markov chain. The built-in Hidden Markov parameter estimation function in MATLAB was utilized to estimate a Markovian transition matrix based on the TRPV4 sparklet data and their corresponding channel opening time course. The estimated transition matrix was modeled as a partially coupled Markov chain, suggesting the coupling coefficient ($\kappa$) values varying from 0 (no coupling or independent gating) to 1 (maximum coupling).

## Immunostaining for AKAP150 and PKG in ECs of the Intact PAs and MAs

Immunostaining assay was performed as described previously.[5] Briefly, mouse intact PAs and MAs cut longitudinally and pinned down on SYLGARD blocks were rapidly fixed with ice-cold acetone for 10 minutes and then washed 3 times with PBS. The arteries were permeabilized with 0.2% Triton-X for 30 minutes, blocked with 5% normal donkey serum (ab7475, Abcam, Cambridge, MA) for 1 hour, and incubated with a goat polyclonal AKAP150 antibody (sc-6445, 1:250, Santa Cruz Biotechnology, Dallas, TX) or a rabbit polyclonal anti-cGKI antibody (ab37709, 1:100, Abcam, Cambridge, MA) overnight at 4°C. After 5 washes with PBS, PAs and MAs were incubated with Alexa Fluor® 568-conjugated donkey anti-goat (A11057, 1:500, Life Technologies, Carlsbad, CA) or anti-rabbit secondary antibody (A10042, 1:500, Life Technologies) for 1 hour at room temperature in a dark room. Immunostaining images were acquired using the Andor imaging system described above. Images were obtained along the *z*-axis from the top of ECs to the bottom of SMCs with a slice size of 0.05 μm. Connective tissue autofluorescence was evaluated by exciting at 488 nm with a solid-state laser and collecting emitted fluorescence with a 525/36-nm band-pass filter. AKAP150 and PKG immunostaining (ie, red-pseudo-color images) was assessed by exciting at 561 nm and collecting emitted fluorescence with a 607/36-nm band-pass filter. The specificity of the antibodies was tested using competing peptides and by substitution with PBS. AKAP150 or PKG-associated staining was absent under these conditions.

## Statistical Analysis

The n number represents the unit of analysis, and has been specified in each figure legend. The data in this article were normally distributed; therefore, parametric statistics were performed and mean±SEM were used to describe the data set. $P<0.05$ was considered significant. The n numbers and *P* values are indicated in each figure legend. Two-tailed, paired (for paired observations) or independent 2-sample *t* test was used for comparisons between 2 groups. One-way ANOVA with post hoc Tukey test (comparing different means) or Dunnett test (comparisons with control group), or 2-way ANOVA with post hoc Tukey test was used for comparing 3 or more groups. Statistical analysis was performed using OriginPro7.5. For all the calculations of TRPV4 sparklet activity per site and activity per field, n value represents number of fields.[4,5] For the coupling coefficient analysis, n value represents number of sites.[5] Only 1 artery from a mouse was used for 1 experimental treatment. Within an experimental treatment group, activity per site did not change significantly among different fields from the same artery ($P>0.05$), or among fields from different arteries as determined using 1-way ANOVA. Moreover, the coupling coefficient values also did not change significantly among different fields from the same artery, or among fields from different arteries under the same experimental treatment group. In some cases, activity per field was calculated instead of activity per site to account for fields with no active sites, and was not significantly different among different arteries from the same experimental treatment group.

## Results

### Native Endothelium From Small PAs Exhibits Unitary TRPV4 Sparklets With Distinct Spatial Properties

We recently discovered localized, unitary $Ca^{2+}$ influx events through TRPV4 channels in the endothelium from small MAs, and termed them TRPV4 sparklets.[4,5] Because of the structural and functional differences between systemic and pulmonary circulations,[6] we hypothesized that TRPV4 sparklets from small PAs exhibit unique biophysical properties. Local $Ca^{2+}$ signals were studied in the intact endothelium from small (≈100–200 μm), fourth-order PAs (Figure 1A, *top panel*). CPA (20 μmol/L, sarcoplasmic/endoplasmic reticulum $Ca^{2+}$-ATPase inhibitor) was used to deplete intracellular

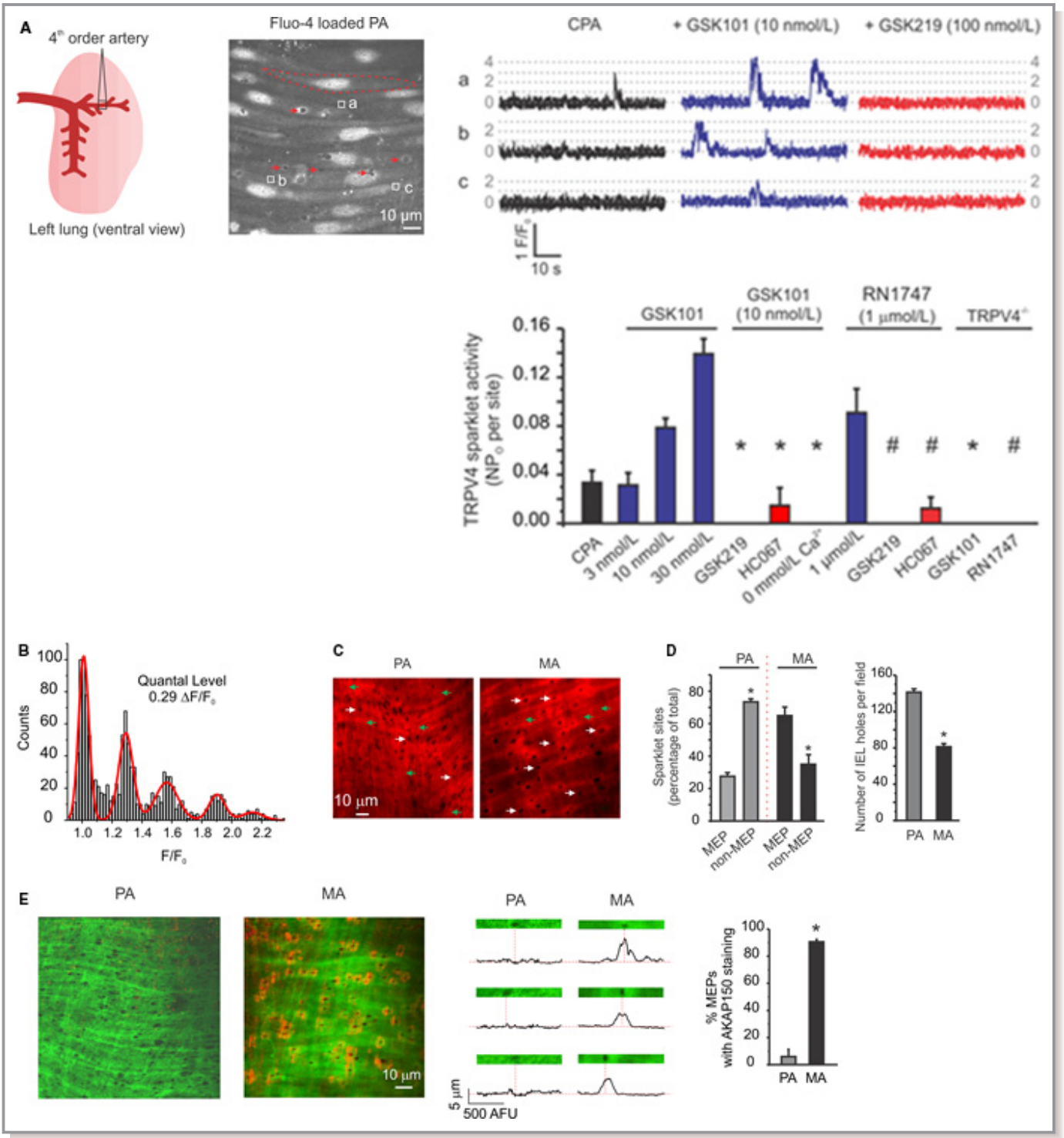

**Figure 1.** Native endothelium from small pulmonary arteries (PAs) displays transient receptor potential vanilloid 4 (TRPV4) sparklets with distinct spatial localization. Local $Ca^{2+}$ influx events through TRPV4 channels (TRPV4 sparklets) were recorded in en face fourth-order PAs and third-order mesenteric arteries (MAs) loaded with fluo-4AM (10 μmol/L). Cyclopiazonic acid (CPA, 20 μmol/L) was used in order to eliminate interference from $Ca^{2+}$ release from the endoplasmic reticulum (ER). A, *Top*, the diagram indicates a fourth-order PA from left lung that was used in this study (*left*). A grayscale image of a field of view with ≈15 endothelial cells (ECs; *right*). The dotted line indicates the outline of a single EC. Square boxes represent the regions of interest (ROIs) placed at the sparklet sites detected within a recording duration of 1 min. Arrows point to the holes in internal elastic lamina (IEL) that represent myoendothelial projections (MEPs). *Middle*, fractional fluorescence ($F/F_0$) traces were obtained from the ROIs shown in the *top* panel. The traces indicate sparklet activity under basal conditions (CPA), with the TRPV4 agonist GSK1016790A (GSK101) alone and in the presence of TRPV4 inhibitor GSK2193784 (GSK219). Dotted lines represent the single-channel levels derived from all-points histogram in (B). *Bottom*, averaged TRPV4 sparklet activity under basal conditions (CPA), in the presence of TRPV4 agonist GSK101, GSK101 in the absence or presence of 2 different TRPV4 channel inhibitors (GSK219, 100 nmol/L and HC067047 or HC067, 1 μmol/L) or 0 mmol/L extracellular $Ca^{2+}$, another TRPV4 channel agonist RN1747 in the absence or presence of TRPV4 inhibitors GSK219 (100 nmol/L) and HC067 (1 μmol/L), and GSK101 (10 nmol/L) and RN1747 (1 μmol/L) in the PAs from $TRPV4^{-/-}$ mice. Data are mean±SEM; TRPV4 sparklet activity ($NP_O$ per site) was calculated using the quantal amplitude derived from (B); N represents the number of channels at a site and $P_O$ is the open state probability of the channels (n=5 fields; $P<0.0001$ using 1-way ANOVA and post hoc Tukey test; * and # indicate statistical significance [$P<0.05$] vs 10 nmol/L GSK101 and 1 μmol/L RN1747, respectively). B, All-points histogram was constructed from $F/F_0$ traces pooled from 3 PAs and was fit with a multi-Gaussian curve. The quantal levels (single-channel amplitudes) were derived from the peaks of the multi-Gaussian curve. C, Experiments were performed in arteries loaded with fluo-4AM and Alexa Fluor 633 hydrazide. Representative images show black holes in the IEL that represent MEPs. Sparklet ROIs were superimposed with IEL staining. Arrows indicate MEP sites in the IEL (white) and non-MEP sites (green) that overlapped with sparklet sites. D, (*Left)* Averaged data for localization of sparklet sites at MEPs in PAs and MAs. Data are mean±SEM (n=10 fields; $P<0.05$ using 2-way ANOVA and post hoc Tukey test; *$P<0.05$ vs MEP). (*Right)* Average number of IEL holes per field in PAs and MAs. Data are mean±SEM (n=10 fields; $P<0.05$ using 2-sample *t* test). E, AKAP150 staining was performed in en face third-order MAs and fourth-order PAs as described in the Methods section. (*Left)* Representative AKAP150 staining images from PAs and MAs, where green color indicates the autofluorescence of the internal elastic lamina (IEL), black holes in the IEL indicate MEPs, and red color indicates AKAP150-staining. (*Middle)* Plot profiles of AKAP150 immunostaining for representative horizontal transects. Dotted lines indicate the positions of MEPs located at the holes in IEL. Images were acquired along the *z*-axis (0.05-μm optical slice). (*Right*) Averaged AKAP150 localization from MAs and PAs; AKAP150 immunostaining within 5 μm from the center of the holes in IEL was considered to be localized at the IEL (n= 5 arteries; *$P<0.0001$ using independent *t* test).



stores of $Ca^{2+}$ and to eliminate the interference from $Ca^{2+}$ release from intracellular stores in en face PAs. In the presence of CPA alone, there were ≈2 TRPV4 sparklet sites per field of view (≈15 ECs, Figure 1A, *top panel*) within a recording duration of 1 minute (Figure S1A). The number of TRPV4 sparklet sites per field was increased 2- and 7-fold by the selective channel agonists, GSK1016790A (GSK101; 3 nmol/L; Video S1) and RN1747 (1 μmol/L), respectively (Figure S1A and S1B). The TRPV4 sparklet activity was almost entirely inhibited by selective TRPV4 inhibitors GSK2193874 (GSK219; 100 nmol/L) and HC067047 (HC067; 1 μmol/L) (Figure 1A, *middle and bottom panels*; Figure S1A). The $Ca^{2+}$ sparklets elicited by GSK101 and RN1747 were absent in arteries from $TRPV4^{-/-}$ mice (Figure 1A, *bottom panel*—Figure S1A). The $Ca^{2+}$ sparklets elicited by GSK101 were immediately abolished as the external $Ca^{2+}$ was changed from 2 to 0 mmol/L (Figure 1A, *bottom panel*; Figure S1C), confirming that the TRPV4 sparklets represented the influx of extracellular $Ca^{2+}$ through TRPV4 channels on EC membrane. Moreover, the increase in fluorescence at a sparklet site was not accompanied by an increase in whole-cell fluorescence (Figure S2), indicating that TRPV4 sparklets did not alter whole-cell $Ca^{2+}$ levels. The surface area encompassed by EC outlines was ≈45-fold higher than the spatial spread of TRPV4 sparklets, further supporting the local nature of sparklets (Figure S2C).

The fractional fluorescence ($F/F_0$) traces revealed square, discrete amplitudes of TRPV4 sparklets, reminiscent of single-channel openings from a patch clamp experiment (Figure 1A, *middle panel*). Therefore, we used the following single-channel opening criteria to determine whether $Ca^{2+}$ sparklets in PAs are unitary events[4,35]: (1) small recording volumes; (2) high $Ca^{2+}$ permeability and single channel conductance; (3) quantal amplitudes; and (4) dependence of the sparklet amplitude on $Ca^{2+}$ electrochemical gradient but not on the concentration of the agonist or inhibitor.[35] Regarding the first criterion, ECs from small PAs are ≈1-μm thick, corresponding to a recording volume of 1.2 fL. TRPV4 channels have been demonstrated to have a large single channel conductance and $Ca^{2+}$ permeability,[36] satisfying the second criterion. A multiple Gaussian fit to all-points histogram of the fractional fluorescence established a stepwise increase in amplitude, with the quantal level being 0.29 $\Delta F/F_0$ for the arteries loaded with fluo-4 (Figure 1B), and 0.19 $\Delta F/F_0$ for the arteries from $GCaMP2^{Cx40}$ mice (Figure S3A, *top*). Increasing the extracellular $Ca^{2+}$ from 2 to 10 mmol/L produced a 70% increase in the quantal level of $Ca^{2+}$ sparklets (Figure S3A, *middle*). Reducing the electrochemical gradient for $Ca^{2+}$ influx by depolarizing EC membranes using 100 mmol/L extracellular $K^+$ decreased the amplitude of these events by 50% (Figure S3A, *bottom*), satisfying the third criterion. Moreover, the quantal

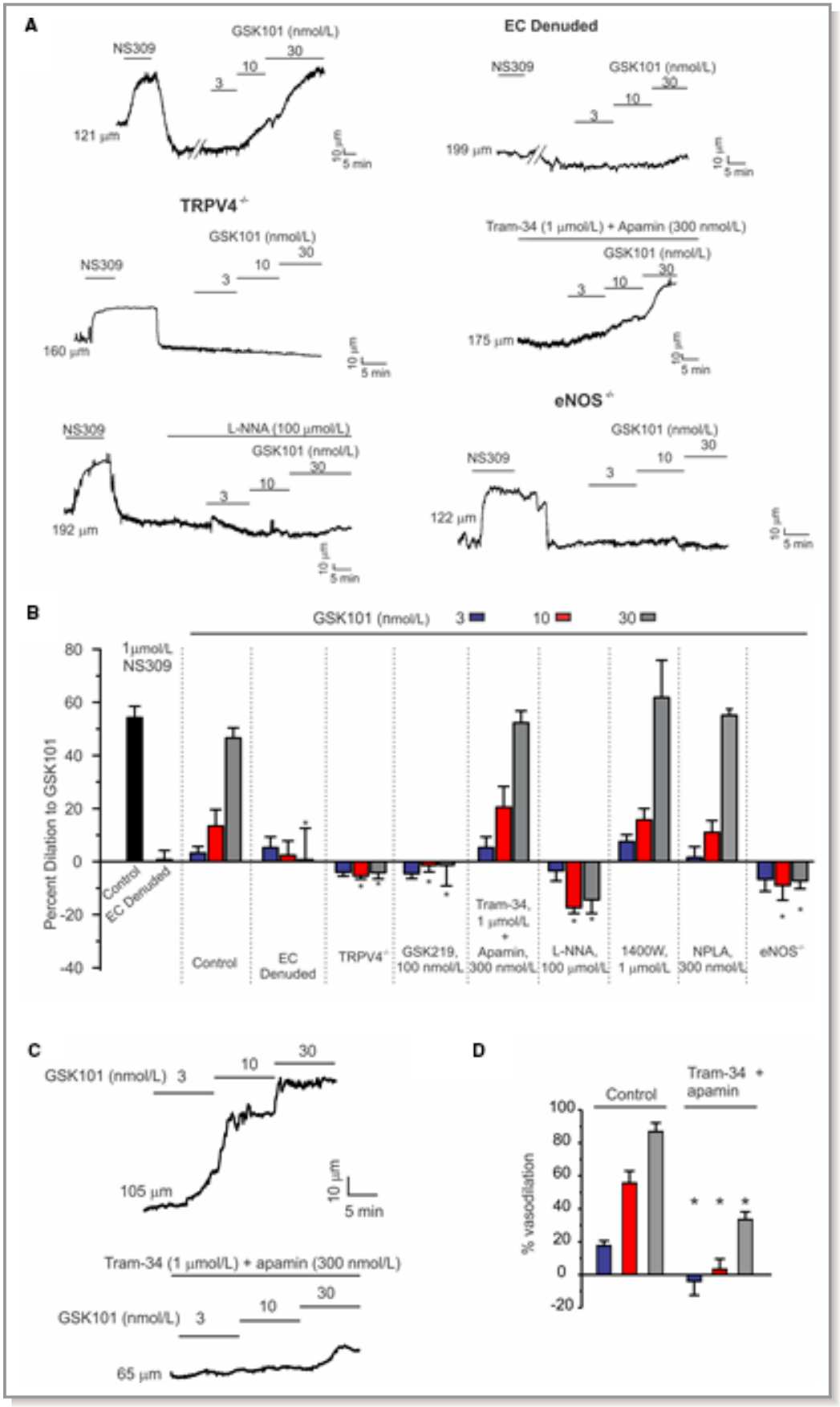

**Figure 2.** TRPV4 channel activation dilates cannulated, pressurized small PAs through endothelial nitric oxide synthase (eNOS) activation, and small MAs through IK/SK channel activation. Fourth-order PAs from left lung were cannulated and pressurized to 15 mm Hg and third-order MAs were pressurized to 80 mm Hg to record the changes in internal diameter. Both PAs and MAs were preconstricted with thromboxane analog U46619 (100 nmol/L). Dilation to NS309 (1 μmol/L), an activator of endothelial IK and SK channels, was used as a criterion to confirm functional viability of the endothelium. A, Representative traces for GSK101-induced vasodilation under control conditions, in the endothelium-denuded PAs, in the PAs from TRPV4$^{-/-}$ mice, in the presence of IK and SK channel inhibitors (Tram-34 and apamin, respectively), NOS inhibitor L-NNA, and in PAs from eNOS$^{-/-}$ mice. Experiments in eNOS$^{-/-}$ mice were performed in the presence of iNOS inhibitor 1400W to account for a possible compensation by iNOS.[42] B, (*left to right*) Averaged diameter responses to NS309 in control (n=37 arteries) and endothelium-denuded (n=5 arteries) PAs, GSK101 in control PAs (n=8 arteries), in endothelium-denuded PAs (n=5 arteries), in PAs from TRPV4$^{-/-}$ mice (n=9 arteries), in the presence of GSK219 (n=4 arteries), Tram-34+apamin (n=9 arteries), L-NNA (n=11 arteries), 1400W (n=5 arteries), NPLA (nNOS inhibitor, n=8 arteries), and in PAs from eNOS$^{-/-}$ mice (n=5 arteries). Data are mean±SEM; $P<0.05$ using 2-way ANOVA and post hoc Tukey test; *$P<0.05$ vs corresponding concentration under control conditions. C, Representative diameter traces for the effect of GSK101 on MA diameter in the absence (*left*) or presence (*right*) of the IK and SK channel inhibitors Tram-34 and apamin, respectively. D, Averaged diameter data for GSK101-induced dilations in the absence or presence of Tram-34 and apamin (n=4 arteries; *$P<0.05$ using 2-way ANOVA and post hoc Tukey test). EC indicates endothelial cell; L-NNA, L-$N^G$-nitroarginine; MAs, mesenteric arteries; NPLA, $N^{\omega}$-Propyl-L-arginine hydrochloride ; PAs, pulmonary arteries; TRPV4, transient receptor potential vanilloid 4.

amplitude did not change with the use of different agonists, with increasing concentration of an agonist, or with the use of TRPV4 inhibitor (Figure S3B), satisfying the fourth criterion. These results supported the concept that TRPV4 sparklets in PA endothelium represent unitary $Ca^{2+}$ influx events through TRPV4 channels.

In small MAs, the majority (≈60%) of TRPV4 sparklet sites occurred at endothelial projections to SMCs or MEPs,[5] where IK channels were also localized.[1,5] In small PAs, however, a small percentage of sparklet sites (25±3%; n=5 PAs) occurred at the MEPs. To confirm the spatial differences in sparklet localization between small PAs and MAs, IEL was stained with Alexa Fluor 633 (a marker for extracellular matrix)[30] immediately after $Ca^{2+}$ imaging experiments. Overlay of sparklet site regions of interest with IEL staining images showed that only ≈28% of the sparklet sites overlapped with MEPs in small PAs, whereas ≈65% of sparklet sites overlapped with MEPs in small MAs (Figure 1C and 1D). The total number of holes per field of view was, however, higher in PAs compared with MAs (Figure 1D). These results established the spatial differences in TRPV4 sparklet activity between small PAs and MAs. We previously showed that MEP-localized A-kinase anchoring protein 150 was required for localization of TRPV4 sparklets at MEPs in MAs. Consistent with the non-MEP localization of sparklets in PAs, only ≈5% of holes in the IEL showed identifiable AKAP150 staining in PAs when compared with ≈90% of the MEPs in MAs (Figure 1E).

## TRPV4 Sparklets Cause Vasodilation in Small PAs via eNOS Activation

Administration of TRPV4 channel agonist GSK101 lowered PAP (pulmonary arterial pressure) in rats.[37] At the level of small PAs, however, the functional effect of endothelial TRPV4 channel activation and the $Ca^{2+}$-sensitive targets have not been identified. PAs are normally exposed to intravascular pressures of 10 to 20 mm Hg. We therefore cannulated and pressurized fourth-order PAs at 15 mm Hg to assess the effect of TRPV4 channel activation on PA diameter. PAs were preconstricted with U46619 (100 nmol/L), a thromboxane A2 receptor agonist (32±2% constriction; n=30 PAs). NS309, a highly specific activator of endothelial IK and SK channels,[38] induced dilations in PAs that were absent in endothelium-denuded PAs, confirming the presence of functional IK and SK channels in PA endothelium (Figure 2A and 2B). PAs were then treated with GSK101 (3–30 nmol/L), which caused a concentration-dependent vasodilation (Figure 2A and 2B). GSK101-induced dilation was absent in endothelium-denuded PAs, PAs from TRPV4$^{-/-}$ mice, and in the presence of TRPV4 channel inhibitor GSK219 (Figure 2A and 2B), confirming that endothelial TRPV4 channel activation dilated small PAs.

We previously showed that endothelial TRPV4 channels induced vasodilation predominantly via activation of IK/SK channels in small MAs constricted by intravascular pressure.[4] Presence of U46619 in the superfusate did not alter the IK/SK channel-dependent nature of TRPV4 channel-induced vasodilation in MAs (Figure 2C and 2D). We, therefore, tested the effect of IK and SK channel inhibitors, Tram-34 (1 μmol/L) and apamin (300 nmol/L), respectively, on TRPV4-vasodilation in small PAs. While NS309-induced vasodilation was reduced by 70.0±10.6% (n=5 PAs) in the presence of Tram-34 and apamin, TRPV4 channel-induced vasodilation was not affected by IK/SK channel inhibitors (Figure 2A and 2B), raising an interesting possibility that a distinct local $Ca^{2+}$ signaling network mediated TRPV4-induced vasodilation in small PAs. Although the activation of eNOS by localized $Ca^{2+}$ signals has not been described, global increase in $Ca^{2+}$ is known to activate eNOS.[39] We, therefore, tested the possibility that TRPV4 sparklets activated eNOS to cause vasodilation in small PAs. Inhibition of NOS with L-NNA constricted PAs by ≈13±1% (n=12 PAs), indicating a tonic influence of NO on basal diameter of PAs. In the presence of L-NNA,

GSK101-induced vasodilation was abolished (Figure 2A and 2B). However, L-NNA is a nonselective inhibitor of eNOS, inducible NOS, and neuronal NOS. To determine the relative contribution from each NOS isoform to TRPV4-vasodilation, we used a selective inducible NOS inhibitor 1400W[40] (1 μmol/L) or a selective neuronal NOS inhibitor *N*ω-propyl-L-arginine hydrochloride[41] (300 nmol/L). In the presence of either of these inhibitors, the TRPV4-vasodilation was not altered (Figure 2A and 2B), pointing to a TRPV4-eNOS signaling network in PAs. The role of eNOS in TRPV4-induced vasodilation was verified by studying TRPV4 dilations in eNOS$^{-/-}$ mice in the presence of 1400W (inducible NOS inhibitor)[40] to account for a possible compensation by inducible NOS.[42] In the PAs from eNOS$^{-/-}$ mice, TRPV4 dilations were absent (Figure 2A and 2B), confirming that TRPV4-vasodilation in PAs was being mediated by eNOS activation.

## TRPV4 Sparklets Regulate NO Release From the Endothelium in PAs but Not in MAs

The eNOS-dependent nature of TRPV4 sparklet-induced vasodilation suggested a local TRPV4-eNOS coupling in small PAs. Because NO generated in ECs can passively diffuse to the SMCs, we postulated that NO levels are increased in both EC and SMC layers following TRPV4 channel activation. NO levels in ECs and SMCs were assessed by recording DAF-FM fluorescence. Spermine NONOate (NONOate, 3–30 μmol/L), a NO donor, caused a concentration-dependent increase in DAF-FM fluorescence in both EC and SMC layers (Figure S4A and S4B), demonstrating that an increase in NO level could be detected with DAF-FM. Both ECs and SMCs showed a low level of basal DAF-FM fluorescence (Figure 3A and 3B). Activation of TRPV4 channels with GSK101 (30 nmol/L) increased DAF-FM fluorescence in EC and SMC layers in small PAs (Figure 3A and 3B). Consistent with the NOS-independent nature of TRPV4-vasodilation in small mesenteric arteries[4] (Figure 2C and 2D), TRPV4 channel activation failed to increase NO levels in ECs and SMCs from MAs (Figure 3C). In PAs, GSK101 produced a 1.8-fold increase in DAF-FM fluorescence in ECs and a 2-fold increase in SMCs (Figure 3C). Pretreatment with L-NNA inhibited the GSK101-induced increases in DAF-FM fluorescence in both ECs and SMCs (Figure 3A through 3C). Moreover, in PAs from eNOS$^{-/-}$ mice, GSK101 was unable to increase DAF-FM fluorescence in ECs or SMCs (Figure 3B). These results support the concept that local TRPV4-eNOS signaling regulates NO levels and endothelium-dependent vasodilation in small PAs.

To test the possibility that TRPV4 sparklets regulate NO release under basal conditions (without TRPV4 agonist) in small PAs, we studied the effect of GSK219 on NO levels. The basal DAF-FM fluorescence in both ECs and SMCs was reduced by ≈30% (Figure 3D, *left*) in the presence of GSK219 supporting TRPV4 regulation of basal eNOS activity in PAs. TRPV4 channels are $Ca^{2+}$-selective channels, but they can also conduct other ions including $Na^+$ and $K^+$.[36] To determine whether $Ca^{2+}$ influx through TRPV4 channels is solely responsible for the regulation of eNOS activity by TRPV4 channels, we studied the effect of TRPV4 activation on NO levels in the presence of 0 mmol/L extracellular $Ca^{2+}$. TRPV4 agonist GSK101 was unable to increase NO levels under these conditions (Figure 3D, *right*), confirming that $Ca^{2+}$ influx through TRPV4 channels activated eNOS in small PAs.

To determine whether TRPV4 sparklets potentiate $Ca^{2+}$ release from the ER in PAs, $Ca^{2+}$ signals were recorded in PAs from mice that express the $Ca^{2+}$ biosensor GCaMP2 selectively in ECs.[27,28] The effect of GSK101 on the activity of $Ca^{2+}$ release events and TRPV4 $Ca^{2+}$ sparklets was studied by utilizing the differences in kinetics between $Ca^{2+}$ release signals from the ER ($Ca^{2+}$ pulsars,[2,4] spikes with duration <300 ms, Figure S5A and S5B)[4] and TRPV4 $Ca^{2+}$ sparklets (discrete, square amplitudes, duration >300 ms, Figure S5A and S5B). $Ca^{2+}$ release signals were unaffected by 0 mmol/L extracellular $Ca^{2+}$ and TRPV4 inhibitor, but were inhibited by CPA (Figure S5C). TRPV4 sparklet activity was unaffected by CPA, but was inhibited by 0 mmol/L extracellular $Ca^{2+}$ and TRPV4 inhibitor. GSK101 stimulated $Ca^{2+}$ sparklet activity, but had no effect on the frequency of $Ca^{2+}$ release events (Figure S5B and S5C), suggesting that $Ca^{2+}$ release from the ER did not contribute to eNOS activation by TRPV4 sparklets.

## NO-Dependent Negative Feedback Loop Limits $Ca^{2+}$ Influx Through TRPV4 Channels in PAs

Studies in expression systems reveal an increase in the activity of TRPV4 channels by *S*-nitrosylation[18] and a decrease by GC-PKG signaling,[19] and NO can activate both these mechanisms. We hypothesized that NO released by TRPV4-eNOS signaling serves as an immediate feedback regulator of TRPV4 channel activity in small PAs. To determine the effect of NO on baseline TRPV4 sparklet activity, PAs were treated with L-NNA (100 μmol/L) in the absence of GSK101. L-NNA produced a 3-fold increase in TRPV4 sparklet activity (Figure 4A), revealing TRPV4 channel inhibition by NO. TRPV4 inhibitor GSK219 completely blocked the L-NNA-induced increase in sparklet activity, confirming the specific inhibition of TRPV4 sparklets by NO (Figure 4A). Consistent with the NOS-independent nature of vasodilation in small MAs, L-NNA did not increase baseline sparklet activity in small MAs (Figure 4A, *right*). For a more detailed analysis of the effect of NO on TRPV4 sparklets in PAs, we increased the open state probability of TRPV4 channels by using a small concentration

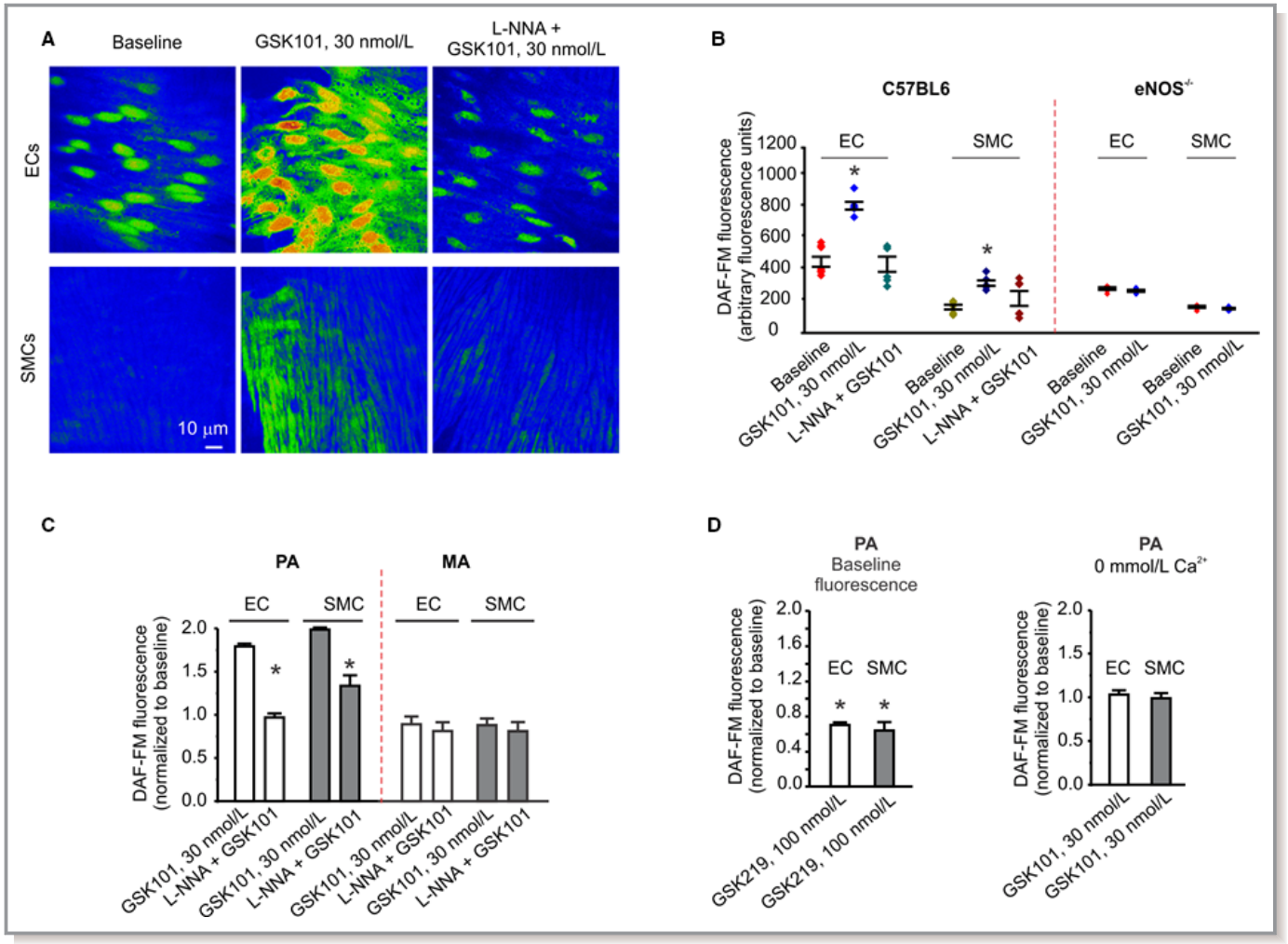


**Figure 3.** TRPV4-eNOS $Ca^{2+}$ signaling mechanism regulates nitric oxide (NO) levels in small PAs. NO levels were recorded in en face fourth-order PAs and third-order MAs loaded with DAF-FM (fluorescent NO indicator; 5 μmol/L). Images were acquired along the *z*-axis using a spinning-disk confocal microscope. A, Representative images for DAF-FM fluorescence in ECs (*top*) and SMCs (*bottom*) of small PAs under basal conditions (*left*), and in the presence of GSK101 (*middle*) alone or with L-NNA (200 μmol/L, *right*). B, Averaged raw fluorescence in ECs and SMCs from PAs of control (*left*) and $eNOS^{-/-}$ mice (*right*); data are mean±SEM; individual data points represent averaged fluorescence of all ECs or SMCs in a field of view (n=6 fields; $P<0.0001$ using 1-way ANOVA and post hoc Dunnett test; $^*P<0.05$ vs the baseline). C, Averaged DAF-FM fluorescence in ECs and SMCs from PAs and MAs relative to the baseline fluorescence (n=6 fields; $^*P<0.0001$ vs GSK101 for PAs using 1-way ANOVA and post hoc Tukey test). D, *Left*, the effect of TRPV4 channel inhibition (GSK219) on baseline DAF-FM fluorescence in both ECs and SMCs from small PAs (n=6 fields; $^*P<0.0001$ vs baseline with independent *t* test); *right*, the increase in DAF-FM fluorescence induced by GSK101 was abolished in the presence of 0 mmol/L extracellular $Ca^{2+}$ (n=6 fields, $P=0.9793$ for ECs and 0.8087 for SMCs using independent *t* test). DAF-FM indicates 4-amino-5 methylamino-2′,7′-difluorofluorescenin diacetate; ECs, endothelial cells; eNOS, endothelial nitric oxide synthase; L-NNA, L-$N^G$-nitroarginine; MAs, mesenteric arteries; PAs, pulmonary arteries; SMCs, smooth muscle cells; TRPV4, transient receptor potential vanilloid 4.

of GSK101 (6 nmol/L). L-NNA also increased sparklet activity in the presence of GSK101 (Figure 4B). To further assess the inhibitory effect of NO on TRPV4 channel function, we examined the effect of NONOate on TRPV4 sparklet activity. At 10 and 30 μmol/L, NONOate increased DAF-FM fluorescence in ECs and SMCs to levels similar to GSK101 (30 nmol/L; Figure S4B). Moreover, PA dilation caused by 30 nmol/L GSK101 was similar to that caused by 10 and 30 μmol/L NONOate (Figure S4C). We therefore used both 10 and 30 μmol/L NONOate for determining the effect of NO on TRPV4 sparklet activity. In the presence of L-NNA, the activity of TRPV4 sparklets was inhibited by ≈2-fold with 10 μmol/L NONOate and by 3-fold with 30 μmol/L NONOate (Figure 4B, *right*) confirming that NO limits $Ca^{2+}$ influx through TRPV4 channels in the endothelium from PAs.

We recently demonstrated that $Ca^{2+}$-dependent cooperative openings of TRPV4 channels amplify $Ca^{2+}$ influx through the channels by 2- to 3-fold in MAs.[4,5] The $F/F_0$ traces for

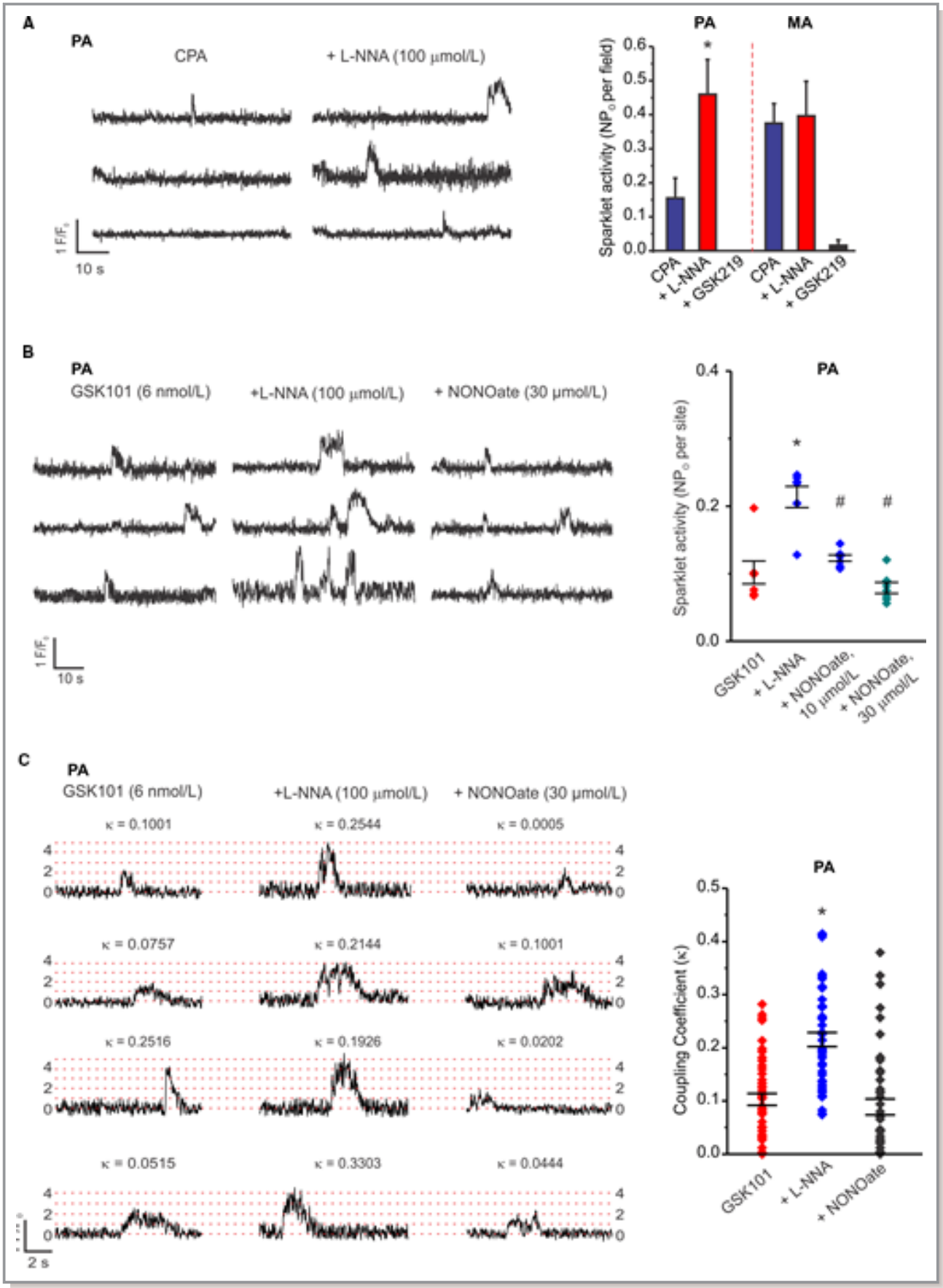

**Figure 4.** Nitric oxide disrupts cooperative openings of TRPV4 channels and lowers channel activity in small PAs. TRPV4 sparklets were recorded in en face fourth-order PAs or third-order MAs loaded with fluo-4AM (10 μmol/L). Cyclopiazonic acid (CPA, 20 μmol/L) was used in order to eliminate the interference from $Ca^{2+}$ release from intracellular stores. L-NNA (100 μmol/L) was used as an inhibitor of NOS and spermine NONOate (NONOate, 10–30 μmol/L) was used as a NO donor. A, Representative $F/F_0$ traces of 3 distinct sparklet sites in a field of view under basal conditions (CPA) and in the presence of L-NNA (*left*) in small PAs. Averaged TRPV4 sparklet activity expressed as $NP_O$ per field, which is a summation of $NP_O$ per site for all the sparklet sites in a field of view. N is the number of channels at a site and $P_O$ is the probability of finding the channel in an open state (n=6 fields; $P<0.05$ using 2-way ANOVA and post hoc Tukey test; $^*P<0.05$ vs CPA) (*right*). B, Representative $F/F_0$ traces from 3 distinct sparklet sites in a field of view in the presence of GSK101, after the addition of L-NNA, and NONOate in the presence of L-NNA (*left*). Averaged TRPV4 sparklet activity ($NP_O$) per site; each data point represents the averaged sparklet activity per site for a field (n=7 fields; $P<0.0001$ using 1-way ANOVA and post hoc Tukey test; $^*P<0.05$ vs GSK101; $^{\#}P<0.05$ vs L-NNA) (*right*). C, To estimate the coupling strength of TRPV4 channels at a sparklet site, we determined coupling coefficients or κ values using coupled Markov Chain model in Matlab. Representative $F/F_0$ traces with corresponding κ values for 4 distinct sparklet sites under control conditions (GSK101), in the presence of L-NNA and in the presence of L-NNA and 30 μmol/L NONOate (*left*). Dotted lines represent the quantal levels derived from all-points histograms. Averaged κ values, data are mean±SEM (n=47 sites; $P<0.0001$ using 1-way ANOVA and post hoc Tukey test; $^*P<0.05$ vs GSK101) (*right*). L-NNA indicates L-$N^G$-nitroarginine; MAs, mesenteric arteries; NONOate, (Z)-1-[N-[3-aminopropyl]-N- [4-(3-aminopropylammonio) butyl]-amino]diazen-1-ium- 1,2-diolate; NOS, nitric oxide synthase; PAs, pulmonary arteries.

TRPV4 sparklets in PAs in the presence of L-NNA displayed simultaneous openings of multiple channels at a site under control conditions, but a lesser number of channels opened simultaneously in the presence of NONOate (Figure 4B), implying that NO may interfere with cooperative openings of TRPV4 channels at a site. Using a coupled Markov chain model in Matlab, we determined coupling coefficients (κ) as an indicator of coupling strength among TRPV4 channels, as we have done previously.[5] The κ values range between 0, which indicates no coupling, and 1, which indicates maximum coupling. Addition of L-NNA increased the coupling strength among TRPV4 channels at a site, and NONOate reduced the coupling strength (Figure 4C). Using an arbitrary cutoff of κ=0.1, ≈50% of the sparklet sites showed coupled openings under control conditions, a number that was increased to 95% in the presence of L-NNA and reduced to 35% by NONOate. These results confirmed that NO disrupted the functional coupling among TRPV4 channels at a site, thereby reducing $Ca^{2+}$ influx in ECs.

## NO Limits $Ca^{2+}$-Dependent Cooperativity of TRPV4 Channels via GC-PKG Signaling

The commonly used inhibitors of *S*-nitrosylation (*N*-acetyl cysteine, dithiothreitol, and ultraviolet light[43]) did not affect the NO-inhibition of TRPV4 channels (Figure 5A), suggesting that *S*-nitrosylation does not play a major role in the NO-inhibition of TRPV4 channels in small PAs. GC-PKG signaling has been shown to inhibit TRPV4 channels in expression systems.[19] We therefore tested the hypothesis that NO activates endothelial GC-PKG signaling to limit $Ca^{2+}$ influx through TRPV4 channels. Both ECs and SMCs from PAs showed a strong expression of PKG (Figure 5B). Similar to L-NNA, GC inhibitor ODQ (3 μmol/L)[44] and PKG inhibitor Rp-8-Br-PET-CGMPS (PET; 30 μmol/L)[45] increased the baseline sparklet activity by ≈2-fold (Figure 5C), confirming that GC-PKG signaling constitutively inhibits TRPV4 channels in PA endothelium. In the presence of GC or PKG inhibitor, L-NNA was unable to further increase the activity of TRPV4 sparklets (Figure 5C, *left*). Moreover, NONOate did not attenuate TRPV4 sparklet activity in the presence of GC or PKG inhibitor (Figure 5C, *right*). GC or PKG inhibitor also enhanced the coupling strength among TRPV4 channels (Figure 5D) by ≈2-fold. In the presence of GC or PKG inhibitors, neither L-NNA nor NONOate (10 and 30 μmol/L) was able to alter the coupling strength among TRPV4 channels at a site (Figure 5D). These results supported the novel concept that in small PAs, NO limits TRPV4 channel activity through GC-PKG signaling in the native endothelium.

$Ca^{2+}$-dependent cooperativity of TRPV4 channels is a key endogenous regulatory mechanism for TRPV4 channel activity.[4,5,20,21] Using EGTA to chelate local $Ca^{2+}$, we previously demonstrated that coupled openings of channels in a cluster were dependent on local increases in $Ca^{2+}$.[5] To determine whether NO-GC-PKG signaling disrupts the functional coupling between the channels by interfering with $Ca^{2+}$-dependent cooperativity, we studied the effect of NONOate on sparklet activity in the presence of EGTA-AM, a cell-permeable form of EGTA. EGTA lowered the sparklet activity and coupling strength among TRPV4 channels in PAs in the presence of L-NNA (Figure 6A and 6B). Moreover, NONOate was unable to further reduce the activity of sparklets and coupling strength among TRPV4 channels in the presence of EGTA (Figure 6A and 6B). Whereas 43% of the total sparklet sites showed cooperative openings (κ>0.1) in the presence of EGTA alone, 41% of the sparklet sites showed cooperative openings after the addition of NONOate in the presence of EGTA, suggesting that NO did not further reduce the cooperativity of TRPV4 sparklets in the presence of EGTA. GSK219, however, was able to cause a further decrease in sparklet activity in the presence of EGTA (n=4 PAs). These results suggest that NO interferes with $Ca^{2+}$-dependent activation of TRPV4 channels, thereby limiting cooperative channel openings.

Based on the NO-GC-PKG negative feedback mechanism for regulating TRPV4 channel activity, we postulated that

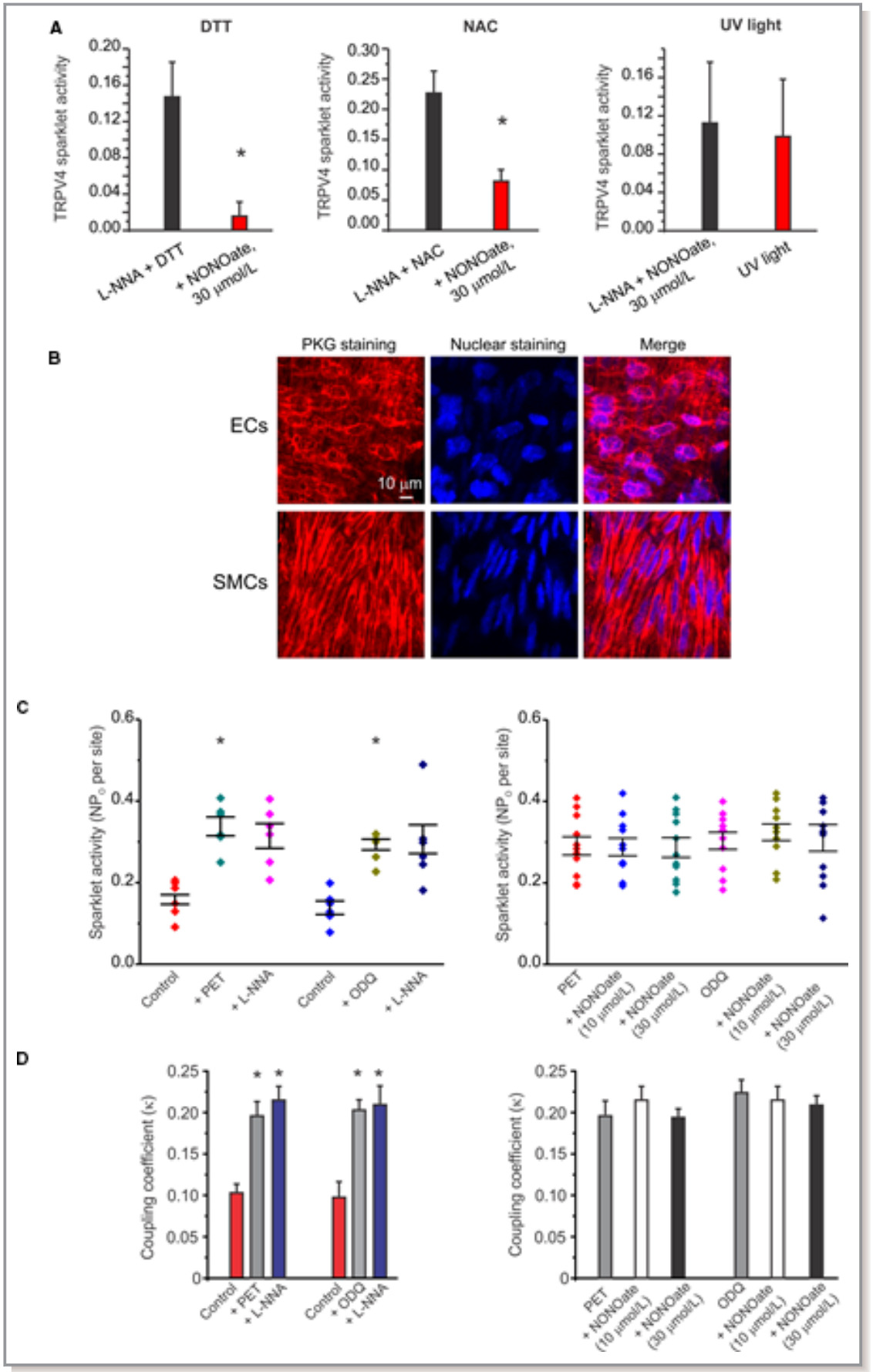

**Figure 5.** Endothelial NO-guanylyl cyclase (GC)-protein kinase G (PKG) signaling disrupts cooperative openings of TRPV4 channels in small PAs. NONOate (30 μmol/L)-induced suppression of TRPV4 sparklet activity was assessed after pharmacological inhibition of *S*-nitrosylation with dithiothreitol (DTT, 1 mmol/L) or *N*-acetyl cysteine (NAC, 5 mmol/L). In addition, ultraviolet (UV) light was applied to physically disrupt serine (S)-NO covalent bonds formed by NO on EC TRPV4 channels. PKG expression and $Ca^{2+}$ signals were recorded in en face fourth-order PAs. TRPV4 sparklets were recorded in small PAs loaded with fluo-4AM (10 μmol/L). The experiments were performed in the presence of CPA (20 μmol/L) to eliminate the interference from $Ca^{2+}$ release from intracellular stores. L-NNA (100 μmol/L) was used as an inhibitor of NOS and spermine NONOate (NONOate, 10–30 μmol/L) was used as a NO donor. To estimate the coupling strength among TRPV4 channels at a sparklet site, we determined coupling coefficients or κ values using a coupled Markov Chain model in Matlab. Cyclopiazonic acid (CPA, 20 μmol/L) was used throughout the experiments to eliminate intracellular $Ca^{2+}$ signaling and exclusively assess $Ca^{2+}$ influx through TRPV4 channels. A, Averaged TRPV4 sparklet activity ($NP_O$ per site) and the effect of NONOate (30 μmol/L) in the presence of DTT (*left*; n=3 fields; **P*=0.0083 using paired *t* test), NAC (*middle*; n=3 fields; **P*=0.0190 using paired *t* test), and after UV exposure (*right*; n=3 fields; *P*=0.8576 using paired *t* test). Data are mean±SEM. B, Representative images for PKG immunostaining (*left*), nuclear staining with DAPI (*middle*) and a merged image (*right*) in the ECs (*top*) and SMCs (*bottom*) from a small PA. The experiments were repeated in 4 small PAs. C, Averaged data indicating the effect of the PKG inhibitor (Rp-8-Br-PET-cGMPS, PET, 30 μmol/L) and the GC inhibitor (ODQ, 3 μmol/L) on TRPV4 sparklet activity, and on L-NNA (100 μmol/L) activation of TRPV4 sparklets (n=6 fields; *P*<0.001 using 1-way ANOVA and post hoc Dunnett test; **P*<0.05 vs control) (*left*). Averaged TRPV4 sparklet activity indicating the effect of NONOate in the presence of PKG (PET) and GC (ODQ) inhibitors (n=10 fields; *P*=0.4708 vs PET or ODQ using 1-way ANOVA and post hoc Dunnett test) (*right*). PET or ODQ were added in the presence of L-NNA (*right panel*), and did not cause a further increase in sparklet activity in the presence of L-NNA. D, Averaged κ values under control conditions (GSK101, 6 nmol/L) and with PET or ODQ before or after the addition of L-NNA (100 μmol/L). Data are mean±SEM (n=47 sites; *P*<0.0001 using 1-way ANOVA and post hoc Dunnett test; **P*<0.05 vs control) (*left*). Averaged κ values in the presence of PET or ODQ before or after the addition of NONOate. Data are mean±SEM (n=47 sites; *P*=0.2315 vs PET or ODQ using 1-way ANOVA and post hoc Dunnett test) (*right*). EC indicates endothelial cells; DAP I4',6-Diamidino-2-Phenylindole, GC, guanylyl cyclase; L-NNA, L-$N^G$-nitroarginine; NAC, *N*-acetyl cysteine; NO, nitric oxide; NONOate, (Z)-1-[N-[3-aminopropyl]-N- [4-(3-aminopropylammonio) butyl]-amino]diazen-1-ium- 1,2-diolate; PAs, pulmonary arteries; PKG, protein kinase; SMCs, smooth muscle cells; TRPV4, transient receptor potential vanilloid 4; UV, ultraviolet.

removing this inhibition would augment TRPV4-vasodilation in PAs. In the presence of GC inhibitor ODQ, the dilation to GSK101 was markedly increased at each concentration (3–30 nmol/L) when compared with vasodilation in the absence of ODQ (Figure 6C and 6D), further supporting the role of NO-GC-PKG negative feedback mechanism as a "limiter" of $Ca^{2+}$ influx through TRPV4 channels and TRPV4-vasodilation in PAs.

## ATP Is an Endogenous Activator of TRPV4 Sparklets in Endothelium From Small PAs

In small mesenteric and cremaster arteries, physiological muscarinic receptor agonist acetylcholine caused vasodilation predominantly through activation of endothelial TRPV4 sparklets.[1,4,5] In small PAs, however, neither muscarinic receptor agonist (carbachol or CCh) nor bradykinin receptor agonist (bradykinin) was able to activate TRPV4 sparklets (Figure S6). Carbachol dilated large PAs (>400 μm), but was unable to evoke dilation in small PAs (Figure 7A), underscoring functional differences in the endothelium from large and small PAs. We, therefore, postulated that TRPV4 channels in ECs from small PAs couple to novel physiological activators. Previous studies in large PAs revealed that endogenous purinergic receptor activator ATP increases endothelial $Ca^{2+}$ and causes endothelium-dependent vasorelaxation.[22–24,46,47] We, therefore, hypothesized that ATP dilates small PAs via activation of TRPV4 sparklets. ATP (10 μmol/L) induced an 8-fold increase in TRPV4 sparklet activity in PAs, an effect that was inhibited by a general P2 purinergic receptor inhibitor suramin and TRPV4 inhibitor GSK219, and was absent in PAs from $TRPV4^{-/-}$ mice (Figure 7B), suggesting P2 purinergic receptor-dependent activation of TRPV4 channels by ATP. In cannulated, pressurized small PAs, ATP (1–10 μmol/L) induced a concentration-dependent dilation, which was inhibited by GSK219 and L-NNA, and was absent in endothelium-denuded PAs and PAs from $TRPV4^{-/-}$ mice (Figure 7C). It is possible that catabolism of ATP to ADP and/or adenosine may activate TRPV4 channels through P2Y1[48] and adenosine receptors, respectively. ADP itself did not induce dilation in PAs (Figure 7D). Adenosine dilated PAs, but this effect was not inhibited by TRPV4 inhibitor, thus ruling out a role for adenosine in ATP-induced vasodilation of PAs (Figure 7E). Taken together, these results reveal that ATP is a novel endogenous activator of local TRPV4-eNOS signaling in small PAs.

## Discussion

Despite the functional differences between systemic and pulmonary circulations, the identity of local $Ca^{2+}$ signals that regulate vascular function in small PAs remains entirely unknown. Our discoveries of spatially distinct TRPV4 sparklets in small PAs and local TRPV4-eNOS signaling network not only support a novel paradigm that eNOS can be activated by spatially restricted $Ca^{2+}$ signals, but also identifies TRPV4 channels as a key regulator of basal and induced eNOS activity in pulmonary microcirculation. Moreover, inhibition of TRPV4 channel cooperativity by NO through GC-PKG signaling represents a novel endogenous mechanism for the regulation of TRPV4 channel function. Although endothelial TRPV4

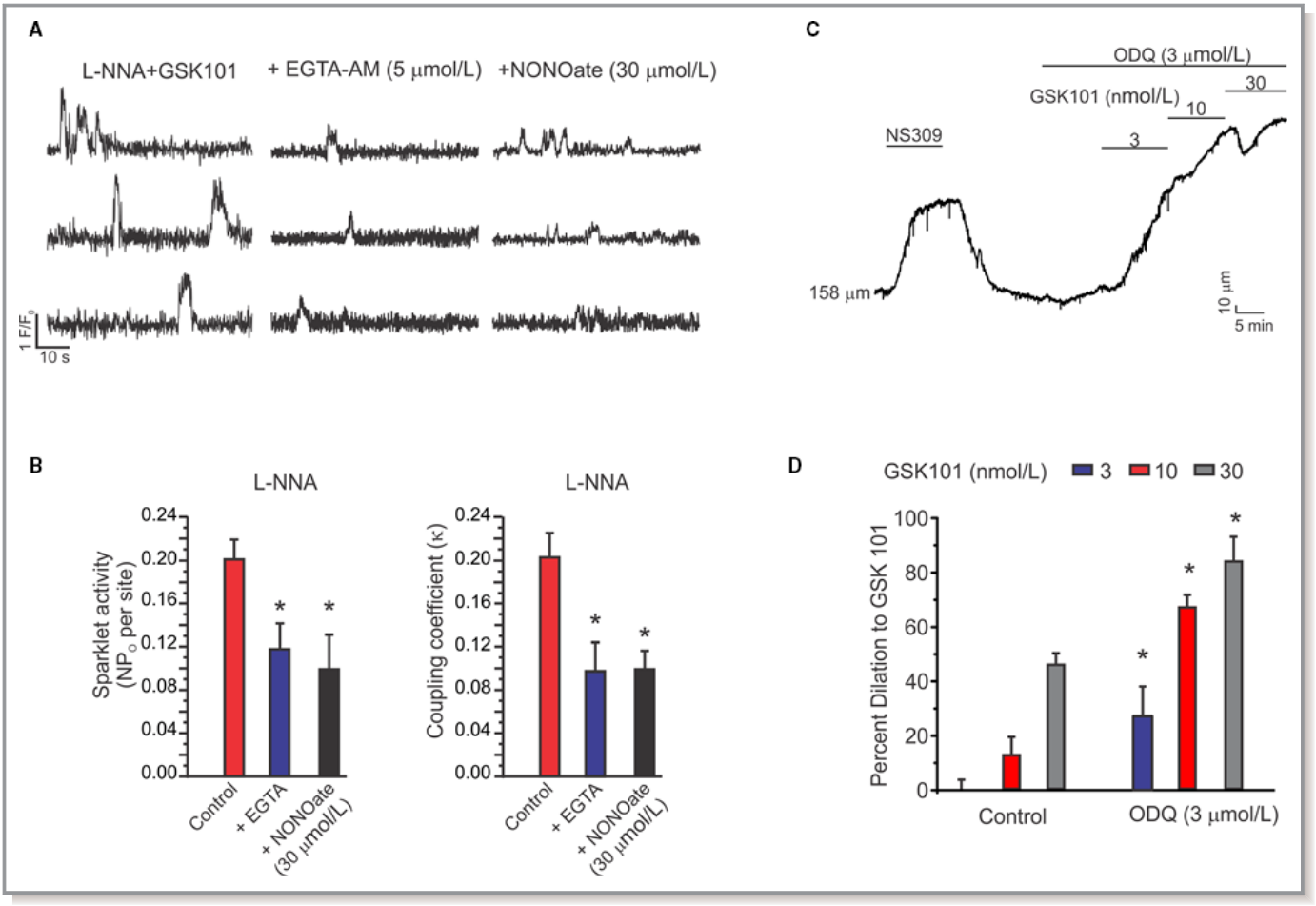


**Figure 6.** NO-GC-PKG signaling impairs $Ca^{2+}$-dependent cooperative openings of TRPV4 channels in small PAs. TRPV4 sparklets were recorded in PAs loaded with fluo-4AM (10 μmol/L). The experiments were performed in the presence of CPA (20 μmol/L) to eliminate the interference from $Ca^{2+}$ release from intracellular stores. L-NNA (100 μmol/L) was used as an inhibitor of NOS and spermine NONOate (NONOate, 10–30 μmol/L) was used as a NO donor. Coupling coefficients or κ values for coupling among TRPV4 channels were determined using a coupled Markov Chain model in Matlab. Changes in internal diameter were recorded in cannulated fourth-order PAs pressurized to 15 mm Hg. A, Experiments were performed in the presence of GSK101 (6 nmol/L) and L-NNA (100 μmol/L). Representative $F/F_0$ traces indicate the effect of membrane-permeable $Ca^{2+}$ chelator EGTA-AM and NONOate in the presence of EGTA-AM on TRPV4 sparklet activity. B, Averaged TRPV4 sparklet activity per site indicating a decrease in sparklet activity with EGTA-AM and lack of effect of NONOate on TRPV4 sparklet activity in the presence of EGTA-AM (n=24 sites; $P<0.0001$ using 1-way ANOVA and post hoc Dunnett test; $^*P<0.05$ vs GSK101 control) (*left*). Averaged κ values, data are mean±SEM (n=24 sites; $P<0.0001$ using 1-way ANOVA; $^*P<0.05$ vs GSK101 control) (*right*). C, A representative diameter trace for GSK101-induced vasodilations in small PAs pretreated with GC inhibitor ODQ (3 μmol/L). D, Averaged percent dilation to GSK101 (3–30 nmol/L) in PAs treated with ODQ (3 μmol/L) compared with control PAs. Data are mean±SEM (n=8 and 4 arteries for control and ODQ, respectively; $P<0.05$ using 2-way ANOVA and post hoc Tukey test; $^*P<0.05$ vs control). CPA indicates cyclopiazonic acid; GC, guanyl cyclase; L-NNA indicates L-$N^G$-nitroarginine; NO, nitric oxide; NONOate, (Z)-1-[N-[3-aminopropyl]-N- [4-(3-aminopropylammonio) butyl]-amino]diazen-1-ium- 1,2-diolate; NOS, nitric oxide synthase; PAs, pulmonary arteries; PKG, protein kinase; TRPV4, transient receptor potential vanilloid 4.



channels have been studied for several years, their physiological roles remain unclear. Our findings of ATP as a novel endogenous activator of TRPV4 channels may prove crucial for deciphering the physiological roles of TRPV4 channels. Because small PAs regulate vascular resistance, TRPV4 channel-induced vasodilation of small PAs may be important for the regulation of pulmonary vascular resistance under normal and disease conditions. Pulmonary vascular disorders, including pulmonary arterial hypertension, are associated with reduced NO bioavailability and loss of endothelial function.[49–51] It is plausible that an impairment in the TRPV4-eNOS signaling results in endothelial dysfunction in these disorders. Inhaled NO represents a major advancement in acute treatment of pulmonary arterial hypertension, but sustained improvements in the clinical outcomes have not been achieved in adult patients.[52] Inhibition of endothelial TRPV4 channels by inhaled NO may contribute to the negative outcome in pulmonary arterial hypertension. Inhibition of TRPV4 channel activity by

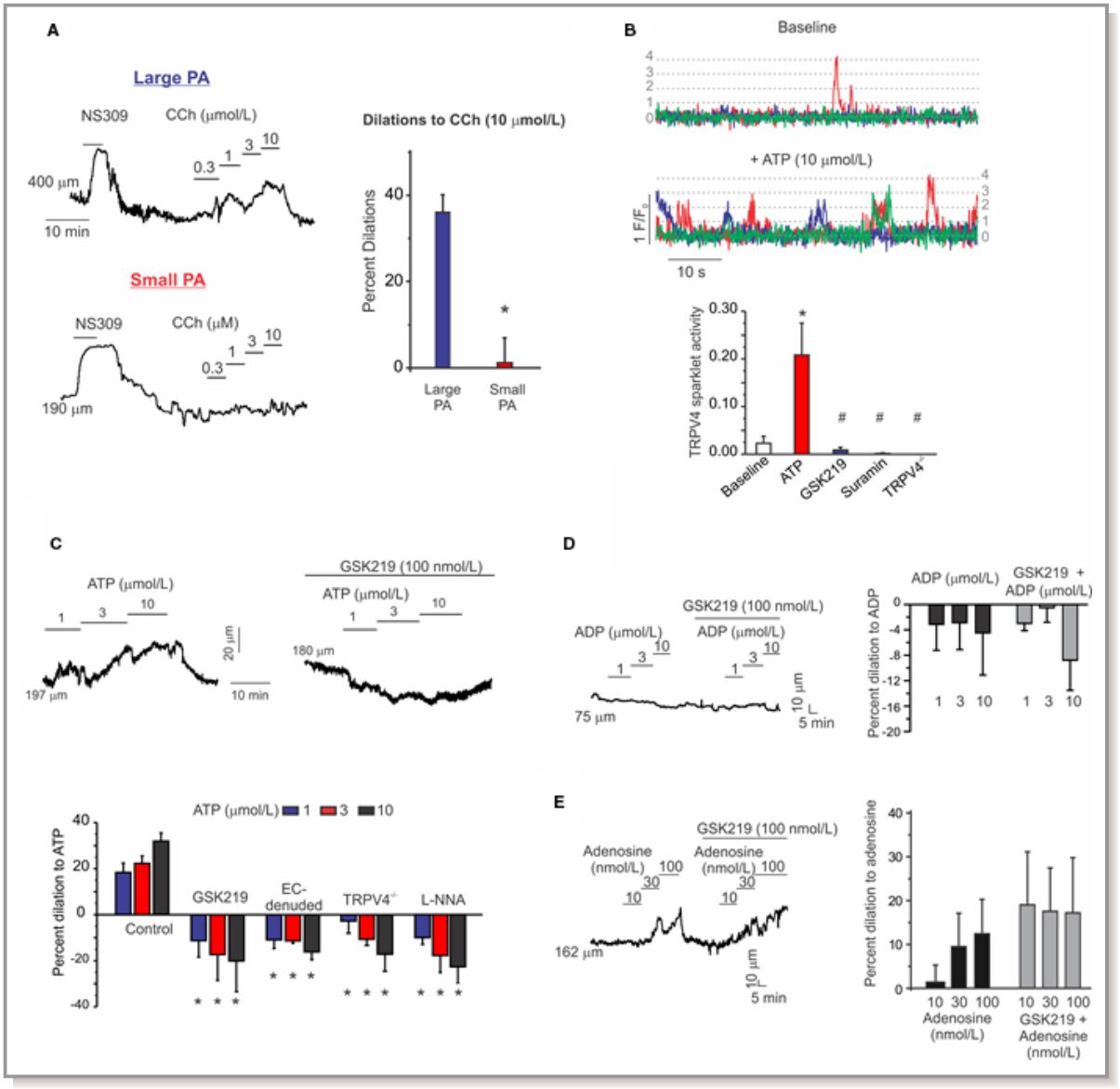


**Figure 7.** ATP is an endogenous activator of local TRPV4-eNOS signaling in small PAs. Changes in internal diameter were recorded in cannulated large PAs and small fourth-order PAs pressurized to 15 mm Hg. TRPV4 sparklets were recorded in en face fourth-order PAs loaded with fluo-4AM (10 μmol/L). CPA (20 μmol/L) was used in order to eliminate the interference from $Ca^{2+}$ release from intracellular stores. A, Representative diameter traces for acetylcholine analog carbachol (CCh)–induced vasodilation in large second-order PAs (≈400 μm, *top left*) and small fourth-order PAs (100–200 μm, *bottom left*). Averaged diameter responses to CCh; data are mean±SEM; (n=5 large PAs, 9 small PAs; **P*<0.01 using independent *t* test) (*right*). B, Representative $F/F_0$ traces of TRPV4 sparklets under baseline conditions (CPA) and with the addition of ATP (10 μmol/L) (*left*). Averaged TRPV4 sparklet activity ($NP_O$) per field of view under basal condition (CPA), in the presence of ATP, ATP in the presence of TRPV4 inhibitor GSK219 (100 nmol/L), P2 purinergic receptor inhibitor suramin (500 μmol/L), or in the PAs from TRPV4$^{-/-}$ mice (n=10 fields; *P*<0.0004 using 1-way ANOVA and post hoc Tukey test; **P*<0.05 vs baseline; $^{\#}P$<0.05 vs ATP) (*right*). C, Representative diameter traces for ATP-induced dilation in fourth-order PAs before (*top left*) and after (*top right*) addition of TRPV4 inhibitor GSK219 (100 nmol/L). (*Bottom*) Averaged percent dilation to ATP (1–10 μmol/L, n=7 arteries) in control PAs, in the presence of GSK219 (n=5 arteries), in EC-denuded PAs (n=5 arteries), in the presence of L-NNA (100 μmol/L, n=6 arteries), and in the PAs from TRPV4$^{-/-}$ mice (n=5 arteries); data are mean±SEM; (*P*<0.05 using 2-way ANOVA and post hoc Tukey test; **P*<0.05 vs control). D, Representative diameter trace (*left*) and averaged data (*right*) for the effect of adenosine diphosphate (ADP) on PA diameter in the absence or presence of TRPV4 inhibitor GSK219 (100 nmol/L; gray; n=5 PAs; *P*>0.05 using 2-way ANOVA and post hoc Tukey test). E, Representative diameter trace (*left*) and averaged diameter data (*right*) for adenosine-induced dilations in the absence or presence of GSK219 (100 nmol/L; gray; n=4 arteries; *P*>0.05 using 2-way ANOVA and post hoc Tukey test). CPA indicates cyclopiazonic acid; eNOS, endothelial nitric oxide synthase; L-NNA, L-$N^G$-nitroarginine; PAs, pulmonary arteries; TRPV4, transient receptor potential vanilloid 4.

NO-GC-PKG signaling will also have implications in the diseases characterized by excessive activation of TRPV4 channels, such as pulmonary edema and lung injury.[53–55]

Previous studies of endothelial $Ca^{2+}$ signals have demonstrated that localized $Ca^{2+}$ signals predominantly activate IK and SK channels to cause vasodilation in small systemic arteries including mesenteric, cremaster, and cerebral arteries.[1–4,56] In small PAs, TRPV4 sparklets preferentially activated eNOS to cause vasodilation. Activation of eNOS by TRPV4 channels was absent in PAs from $eNOS^{-/-}$ mice (Figure 3B), was inhibited by TRPV4 channel inhibitor (Figure 3D, *left*), and required influx of extracellular $Ca^{2+}$ (Figure 3, *right*). TRPV4 sparklets did not activate $Ca^{2+}$ release from intracellular stores (Figure S5C). Additionally, all the $Ca^{2+}$ influx signals in response to TRPV4 channel agonist were inhibited by TRPV4 channel inhibitor and were absent in PAs from $TRPV4^{-/-}$ mice (Figure 1A). These results, in combination with the local nature of TRPV4 sparklets, support a direct activation of eNOS by TRPV4 sparklets.

Selective coupling of TRPV4 sparklets with eNOS for vasodilation in small PAs supports differential $Ca^{2+}$ signaling networks in small PAs and mesenteric/cremaster/cerebral arteries. Our data suggest that the presence of U46619 alone (Figure 2C and 2D) does not alter the IK/SK channel-dependent nature of TRPV4-vasodilation in MAs. The differences in signaling pathways may arise from drastic physiological differences in intravascular pressures in pulmonary and systemic circulations. The pressures used in this study mimicked the physiological intravascular pressures of the 2 vascular beds. Localization of $Ca^{2+}$ signals and IK/SK channels at MEPs has been proposed as a mechanism for preferential activation of IK/SK channels by TRPV4 sparklets in small MAs and cremaster arterioles.[1,2] The non-MEP localization of sparklets in small PAs is consistent with the IK/SK channel-independent nature of TRPV4-vasodilation in small PAs; however, the molecular mechanism underlying preferential TRPV4-eNOS coupling in PAs is not clear. In MAs, the MEP-localization of TRPV4 sparklet activity is attributed to A-kinase anchoring protein 150 (AKAP150)-mediated cooperative opening of TRPV4 channels at the MEPs.[5] Surprisingly, AKAP150 staining was not observed at the MEPs in PAs (Figure 1E), and only a small fraction of TRPV4 sparklets occurred at the MEPs (Figure 1D). Caveolin, a major structural protein of caveolae, directly interacts with and inhibits eNOS activity.[57] Endothelial hemoglobin-α and cytochrome b5 reductase 3 (CytB5R3) have also been shown to regulate the effects of NO on vascular reactivity.[58] It is, therefore, conceivable that differential expression of caveolin, hemoglobin-α, and CytB5R3, along with the absence of AKAP150, is responsible for selective activation of eNOS over IK/SK channels in small PAs. Additionally, differences in the aforementioned mechanisms could be responsible for species-, vessel size-, and vascular bed-specific coupling of TRPV4 sparklets with their signaling targets.

Although TRPV4 channels have been proposed as a key $Ca^{2+}$ influx pathway in vascular endothelium, their endogenous activators remain elusive. The discovery of ATP as an endogenous activator of TRPV4-eNOS signaling may be a crucial step towards deciphering the physiological and pathological roles of TRPV4 channels in the pulmonary circulation. Purinergic signaling is an essential component to the pulmonary vasculature,[59–63] and ATP activation of TRPV4 channels represents a mechanism that may link physiological stimuli to the regulation of pulmonary vascular function. ATP can be released from sympathetic nerves during synaptic transmission, or can be released into the circulation by ECs, SMCs, or erythrocytes.[25,26,64,65] Shear stress, which is a well-known activator of endothelial TRPV4 channels,[66–68] also induces the release of ATP,[65] suggesting a possible involvement of P2 purinergic receptor-TRPV4 signaling in flow-induced vasodilation. Endothelial Gq-protein coupled receptor agonists carbachol and bradykinin activated TRPV4 channels through a phospholipase C-diacylglycerol-protein kinase C mechanism in MAs.[5] ATP may also activate endothelial TRPV4 channels through Gq-coupled P2 purinergic receptors, a possibility that will be explored in future studies.

While TRPV4 channels play a physiologically important role at a low level of activation, excessive TRPV4 channel activity can cause $Ca^{2+}$ overload and EC death.[4] In this context, a dual role for NO—as a mediator of TRPV4-vasodilation and as a limiter of TRPV4 channel activity—provides a more precise control over channel activation and vasodilation. Prior studies in the expression systems reveal 2 possibilities for the modulation of TRPV4 channel function by NO: an increase in channel activity by *S*-nitrosylation,[18] and a decrease in channel activity by GC-PKG signaling.[19] Although *S*-nitrosylation and activation of TRPV4 channels by NO cannot be ruled out, our results suggest that NO-induced TRPV4 channel inhibition via GC-PKG pathway predominates in intact PAs. Unlike PKG, protein kinase A and protein kinase C activation potentiates TRPV4 channel function via channel phosphorylation.[69] These findings point to an interesting possibility that PKG phosphorylates the channel at a site that is different from protein kinase C or protein kinase A phosphorylation, and results in channel inhibition. Previous studies by Yin et al[17] using Fura-2 indicated that NO-cGMP signaling lowers TRPV4-induced increases in global $Ca^{2+}$ levels in lung venular capillary endothelium. Whether this effect of NO is because of a direct effect on single channel function of TRPV4 channels remains unknown. Moreover, a functional effect of NO on TRPV4 channel-induced vasodilation of small PAs is not known. The effect of NO-GC-PKG signaling on $Ca^{2+}$-dependent cooperative openings of TRPV4 channels represents a novel mechanism to control the diameter of small PAs in response to TRPV4 channel activation. How PKG phosphorylation of TRPV4 channel

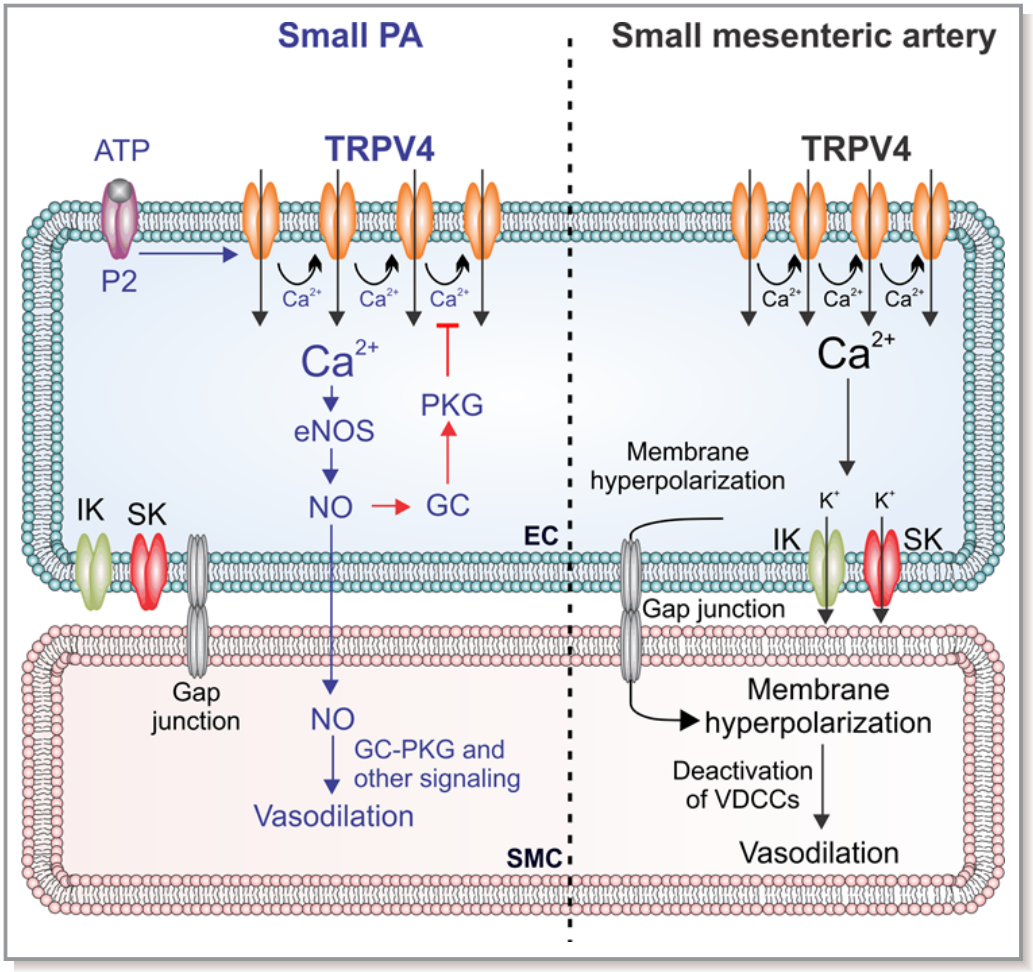


**Figure 8.** Local TRPV4 channel-dependent $Ca^{2+}$ signaling regulates endothelium-dependent vasodilation in resistance-sized PAs. The diagram depicts TRPV4 channel-dependent endothelial $Ca^{2+}$ signaling mechanisms in small PAs and small mesenteric arteries.[1,4,7] In small PAs, TRPV4 sparklets promote eNOS activity and NO release. P2 purinergic receptor agonist ATP is an endogenous activator of the TRPV4-eNOS signaling in PAs. Endothelium-derived NO then causes vasodilation through the activation of SMC guanylyl cyclase (GC)-protein kinase G (PKG) signaling and GC-PKG-independent mechanisms. Blue arrows indicate this pathway. NO also induces activation of endothelial GC-PKG signaling, which lowers $Ca^{2+}$-dependent cooperative opening of TRPV4 channels and limits TRPV4-mediated vasodilations. This pathway is indicated by red arrows. In small mesenteric arteries, TRPV4 $Ca^{2+}$ sparklets selectively activate endothelial IK and SK channels, which hyperpolarize EC and SMC membranes. SMC membrane hyperpolarization deactivates voltage-dependent $Ca^{2+}$ channels (VDCCs), which results in vasodilation, as described earlier. EC indicates endothelial cells; eNOS, endothelial nitric oxide synthase; NO, nitric oxide; PAs, pulmonary arteries; PKG, protein kinase G; SMC, smooth muscle cell; TRPV4, transient receptor potential vanilloid 4.[4]

inhibits the coupling among TRPV4 channels is not known, but 1 possible mechanism could be inhibition of $Ca^{2+}$ potentiation of the channel, thereby limiting the effect of $Ca^{2+}$ on channel cooperativity. In support of this claim, our results demonstrate that in the presence of $Ca^{2+}$ chelator EGTA, which limits TRPV4 channel cooperativity,[5] NO had no effect on channel activity (Figure 6).

Our results also point to distinct functional roles of GC-cGMP-PKG signaling pathways from ECs and SMCs (Figure 8). Activation of the canonical GC-PKG pathway in SMCs leads to vasodilation.[70] Indeed, SMC GC has been targeted to dilate PAs and reduce pulmonary vascular resistance in pulmonary arterial hypertension.[71] Interestingly, the finding that the endothelial GC-PKG pathway has an inhibitory effect on vasodilation suggests that EC and SMC pathways work in opposite directions, and excessive activation of endothelial GC-PKG signaling could lead to increased vasoconstriction and vascular resistance under pathological conditions. Moreover, the finding that GC inhibitor did not inhibit the vasodilation caused by EC-derived NO (Figure 6C and 6D) suggests that in small PAs there

is a vasodilatory component that is activated by NO and that acts independently of the SMC GC-PKG signaling.

In conclusion, our results represent the first direct evidence that localized $Ca^{2+}$ signals regulate NO release in small PAs. Reduced NO bioavailability is a major contributor to endothelial dysfunction in many pulmonary vascular disorders including pulmonary arterial hypertension. The perturbations of TRPV4-eNOS pathway may provide a mechanistic explanation for reduced NO levels and endothelial dysfunction in these disorders. Our results also reveal a potent inhibitory role of NO on TRPV4 channel function, defining it as a novel physiological regulator (limiter) of TRPV4 channels (Figure 8). TRPV4 channels are $Ca^{2+}$-selective cation channels with a large single channel conductance; the amount of $Ca^{2+}$ entering through 1 TRPV4 channel is ≈100 times higher than an L-type $Ca^{2+}$ channel.[72] A slight overactivation of TRPV4 channels could lead to $Ca^{2+}$ overload. It is, therefore, critical to tightly control the activity of these channels without inhibiting their physiological effect. The TRPV4-eNOS signaling achieves this feat by mediating the functional effect of TRPV4 channels, and by limiting the channel function through endothelial GC-PKG signaling. While some pulmonary vascular disorders show reduced NO levels,[10,50,51,73] others show excessive TRPV4 channel activity.[53–55,74,75] Thus, we propose that abnormalities in the NO-PKG-TRPV4 feedback mechanism may be involved in both types of pulmonary dysfunctions.

## Acknowledgments

We would like to acknowledge GlaxoSmithKline for providing TRPV4$^{-/-}$ breeder mice, Dr Adrian Bonev (University of Vermont) for SparkAn, Dr Luis F. Santana (University of California, Davis) for providing the software program for determining coupling coefficients, and Dr Avril Somlyo for her comments on the manuscript.

## Sources of Funding

This work was funded by grants from NIH to Sonkusare (HL121484 and HL138496), Marziano (4T32HL007284), Isakson (HL088554), UVA School of Medicine, and Robert M. Berne Cardiovascular Research Center startup funds to Sonkusare, and American Heart Association predoctoral Fellowship (17PRE33660762) to Marziano.

## Disclosures

None.

## References

1. Bagher P, Beleznai T, Kansui Y, Mitchell R, Garland CJ, Dora KA. Low intravascular pressure activates endothelial cell TRPV4 channels, local Ca2+ events, and IKCa channels, reducing arteriolar tone. *Proc Natl Acad Sci USA*. 2012;109:18174–18179.
2. Ledoux J, Taylor MS, Bonev AD, Hannah RM, Solodushko V, Shui B, Tallini Y, Kotlikoff MI, Nelson MT. Functional architecture of inositol 1,4,5-trisphosphate signaling in restricted spaces of myoendothelial projections. *Proc Natl Acad Sci USA*. 2008;105:9627–9632.
3. Pires PW, Sullivan MN, Pritchard HA, Robinson JJ, Earley S. Unitary TRPV3 channel $Ca^{2+}$ influx events elicit endothelium-dependent dilation of cerebral parenchymal arterioles. *Am J Physiol Heart Circ Physiol*. 2015;309:H2031–H2041.
4. Sonkusare SK, Bonev AD, Ledoux J, Liedtke W, Kotlikoff MI, Heppner TJ, Hill-Eubanks DC, Nelson MT. Elementary $Ca^{2+}$ signals through endothelial TRPV4 channels regulate vascular function. *Science*. 2012;336:597–601.
5. Sonkusare SK, Dalsgaard T, Bonev AD, Hill-Eubanks DC, Kotlikoff MI, Scott JD, Santana LF, Nelson MT. AKAP150-dependent cooperative TRPV4 channel gating is central to endothelium-dependent vasodilation and is disrupted in hypertension. *Sci Signal*. 2014;7:ra66.
6. Gil J. Microcirculation of the lung: functional and anatomic aspects. In: Yuan JX, Garcia JG, Hales CA, Rich S, Archer SL, West JB, eds. *Textbook of Pulmonary Vascular Disease*. New York: Springer; 2010:13–24.
7. Zhang L, Papadopoulos P, Hamel E. Endothelial TRPV4 channels mediate dilation of cerebral arteries: impairment and recovery in cerebrovascular pathologies related to Alzheimer's disease. *Br J Pharmacol*. 2013;170:661–670.
8. Blum-Johnston C, Thorpe RB, Wee C, Romero M, Brunelle A, Blood Q, Wilson R, Blood AB, Francis M, Taylor MS, Longo LD, Pearce WJ, Wilson SM. Developmental acceleration of bradykinin-dependent relaxation by prenatal chronic hypoxia impedes normal development after birth. *Am J Physiol Lung Cell Mol Physiol*. 2016;310:L271–L286.
9. Fike CD, Slaughter JC, Kaplowitz MR, Zhang Y, Aschner JL. Reactive oxygen species from NADPH oxidase contribute to altered pulmonary vascular responses in piglets with chronic hypoxia-induced pulmonary hypertension. *Am J Physiol Lung Cell Mol Physiol*. 2008;295:L881–L888.
10. Klinger JR, Abman SH, Gladwin MT. Nitric oxide deficiency and endothelial dysfunction in pulmonary arterial hypertension. *Am J Respir Crit Care Med*. 2013;188:639–646.
11. Mam V, Tanbe AF, Vitali SH, Arons E, Christou HA, Khalil RA. Impaired vasoconstriction and nitric oxide-mediated relaxation in pulmonary arteries of hypoxia- and monocrotaline-induced pulmonary hypertensive rats. *J Pharmacol Exp Ther*. 2010;332:455–462.
12. Zhang RZ, Yang Q, Yim AP, Huang Y, He GW. Role of NO and EDHF-mediated endothelial function in the porcine pulmonary circulation: comparison between pulmonary artery and vein. *Vascul Pharmacol*. 2006;44:183–191.
13. Harraz OF, Brett SE, Welsh DG. Nitric oxide suppresses vascular voltage-gated T-type $Ca^{2+}$ channels through cGMP/PKG signaling. *Am J Physiol Heart Circ Physiol*. 2014;306:H279–H285.
14. Hu H, Chiamvimonvat N, Yamagishi T, Marban E. Direct inhibition of expressed cardiac L-type $Ca^{2+}$ channels by S-nitrosothiol nitric oxide donors. *Circ Res*. 1997;81:742–752.
15. Lohman AW, Weaver JL, Billaud M, Sandilos JK, Griffiths R, Straub AC, Penuela S, Leitinger N, Laird DW, Bayliss DA, Isakson BE. S-nitrosylation inhibits pannexin 1 channel function. *J Biol Chem*. 2012;287:39602–39612.
16. Mistry DK, Garland CJ. Nitric oxide (NO)-induced activation of large conductance $Ca^{2+}$-dependent $K^{+}$ channels (BK(Ca)) in smooth muscle cells isolated from the rat mesenteric artery. *Br J Pharmacol*. 1998;124:1131–1140.
17. Yin J, Hoffmann J, Kaestle SM, Neye N, Wang L, Baeurle J, Liedtke W, Wu S, Kuppe H, Pries AR, Kuebler WM. Negative-feedback loop attenuates hydrostatic lung edema via a cGMP-dependent regulation of transient receptor potential vanilloid 4. *Circ Res*. 2008;102:966–974.
18. Yoshida T, Inoue R, Morii T, Takahashi N, Yamamoto S, Hara Y, Tominaga M, Shimizu S, Sato Y, Mori Y. Nitric oxide activates TRP channels by cysteine S-nitrosylation. *Nat Chem Biol*. 2006;2:596–607.
19. Du J, Wong WY, Sun L, Huang Y, Yao X. Protein kinase G inhibits flow-induced $Ca^{2+}$ entry into collecting duct cells. *J Am Soc Nephrol*. 2012;23:1172–1180.
20. Parikh J, Kapela A, Tsoukias NM. Stochastic model of endothelial TRPV4 calcium sparklets: effect of bursting and cooperativity on EDH. *Biophys J*. 2015;108:1566–1576.
21. Welsh DG. TRPV4 channel cooperativity in the resistance vasculature. *Biophys J*. 2015;108:1312–1313.
22. Greenberg B, Rhoden K, Barnes PJ. Endothelium-dependent relaxation of human pulmonary arteries. *Am J Physiol*. 1987;252:H434–H438.
23. Konduri GG, Mital S. Adenosine and ATP cause nitric oxide-dependent pulmonary vasodilation in fetal lambs. *Biol Neonate*. 2000;78:220–229.
24. Paffett ML, Naik JS, Riddle MA, Menicucci SD, Gonzales AJ, Resta TC, Walker BR. Altered membrane lipid domains limit pulmonary endothelial calcium entry following chronic hypoxia. *Am J Physiol Heart Circ Physiol*. 2011;301:H1331–H1340.

25. Lohman AW, Billaud M, Isakson BE. Mechanisms of ATP release and signalling in the blood vessel wall. *Cardiovasc Res*. 2012;95:269–280.
26. Sprague RS, Ellsworth ML. Erythrocyte-derived ATP and perfusion distribution: role of intracellular and intercellular communication. *Microcirculation*. 2012;19:430–439.
27. Tallini YN, Brekke JF, Shui B, Doran R, Hwang SM, Nakai J, Salama G, Segal SS, Kotlikoff MI. Propagated endothelial $Ca^{2+}$ waves and arteriolar dilation in vivo: measurements in Cx40BAC GCaMP2 transgenic mice. *Circ Res*. 2007;101:1300–1309.
28. Tallini YN, Ohkura M, Choi BR, Ji G, Imoto K, Doran R, Lee J, Plan P, Wilson J, Xin HB, Sanbe A, Gulick J, Mathai J, Robbins J, Salama G, Nakai J, Kotlikoff MI. Imaging cellular signals in the heart in vivo: cardiac expression of the high-signal $Ca^{2+}$ indicator GCaMP2. *Proc Natl Acad Sci USA*. 2006;103:4753–4758.
29. Villalba N, Sonkusare SK, Longden TA, Tran TL, Sackheim AM, Nelson MT, Wellman GC, Freeman K. Traumatic brain injury disrupts cerebrovascular tone through endothelial inducible nitric oxide synthase expression and nitric oxide gain of function. *J Am Heart Assoc*. 2014;3:e001474. DOI: 10.1161/JAHA.114.001474.
30. Clifford PS, Ella SR, Stupica AJ, Nourian Z, Li M, Martinez-Lemus LA, Dora KA, Yang Y, Davis MJ, Pohl U, Meininger GA, Hill MA. Spatial distribution and mechanical function of elastin in resistance arteries: a role in bearing longitudinal stress. *Arterioscler Thromb Vasc Biol*. 2011;31:2889–2896.
31. Cheng EP, Yuan C, Navedo MF, Dixon RE, Nieves-Cintron M, Scott JD, Santana LF. Restoration of normal L-type $Ca^{2+}$ channel function during Timothy syndrome by ablation of an anchoring protein. *Circ Res*. 2011;109:255–261.
32. Chung SH, Kennedy RA. Coupled Markov chain model: characterization of membrane channel currents with multiple conductance sublevels as partially coupled elementary pores. *Math Biosci*. 1996;133:111–137.
33. Moreno CM, Dixon RE, Tajada S, Yuan C, Opitz-Araya X, Binder MD, Santana LF. Ca(2+) entry into neurons is facilitated by cooperative gating of clustered CaV1.3 channels. *Elife*. 2016;5:e15744.
34. Navedo MF, Cheng EP, Yuan C, Votaw S, Molkentin JD, Scott JD, Santana LF. Increased coupled gating of L-type $Ca^{2+}$ channels during hypertension and Timothy syndrome. *Circ Res*. 2010;106:748–756.
35. Parker I, Smith IF. Recording single-channel activity of inositol trisphosphate receptors in intact cells with a microscope, not a patch clamp. *J Gen Physiol*. 2010;136:119–127.
36. Everaerts W, Nilius B, Owsianik G. The vanilloid transient receptor potential channel TRPV4: from structure to disease. *Prog Biophys Mol Biol*. 2010;103:2–17.
37. Pankey EA, Zsombok A, Lasker GF, Kadowitz PJ. Analysis of responses to the TRPV4 agonist GSK1016790A in the pulmonary vascular bed of the intact-chest rat. *Am J Physiol Heart Circ Physiol*. 2014;306:H33–H40.
38. Leuranguer V, Gluais P, Vanhoutte PM, Verbeuren TJ, Feletou M. Openers of calcium-activated potassium channels and endothelium-dependent hyperpolarizations in the guinea pig carotid artery. *Naunyn Schmiedebergs Arch Pharmacol*. 2008;377:101–109.
39. Fleming I, Busse R. Signal transduction of eNOS activation. *Cardiovasc Res*. 1999;43:532–541.
40. Garvey EP, Oplinger JA, Furfine ES, Kiff RJ, Laszlo F, Whittle BJ, Knowles RG. 1400W is a slow, tight binding, and highly selective inhibitor of inducible nitric-oxide synthase in vitro and in vivo. *J Biol Chem*. 1997;272:4959–4963.
41. Zhang HQ, Fast W, Marletta MA, Martasek P, Silverman RB. Potent and selective inhibition of neuronal nitric oxide synthase by N omega-propyl-L-arginine. *J Med Chem*. 1997;40:3869–3870.
42. Cook S, Vollenweider P, Menard B, Egli M, Nicod P, Scherrer U. Increased eNO and pulmonary iNOS expression in eNOS null mice. *Eur Respir J*. 2003;21:770–773.
43. Hess DT, Matsumoto A, Nudelman R, Stamler JS. S-nitrosylation: spectrum and specificity. *Nat Cell Biol*. 2001;3:E46–E49.
44. Pankey EA, Kassan M, Choi SK, Matrougui K, Nossaman BD, Hyman AL, Kadowitz PJ. Vasodilator responses to acetylcholine are not mediated by the activation of soluble guanylate cyclase or TRPV4 channels in the rat. *Am J Physiol Heart Circ Physiol*. 2014;306:H1495–H1506.
45. Qi H, Zheng X, Qin X, Dou D, Xu H, Raj JU, Gao Y. Protein kinase G regulates the basal tension and plays a major role in nitrovasodilator-induced relaxation of porcine coronary veins. *Br J Pharmacol*. 2007;152:1060–1069.
46. Konduri GG, Bakhutashvili I, Frenn R, Chandrasekhar I, Jacobs ER, Khanna AK. P2Y purine receptor responses and expression in the pulmonary circulation of juvenile rabbits. *Am J Physiol Heart Circ Physiol*. 2004;287:H157–H164.
47. Sprague RS, Olearczyk JJ, Spence DM, Stephenson AH, Sprung RW, Lonigro AJ. Extracellular ATP signaling in the rabbit lung: erythrocytes as determinants of vascular resistance. *Am J Physiol Heart Circ Physiol*. 2003;285:H693–H700.
48. Leon C, Hechler B, Vial C, Leray C, Cazenave JP, Gachet C. The P2Y1 receptor is an ADP receptor antagonized by ATP and expressed in platelets and megakaryoblastic cells. *FEBS Lett*. 1997;403:26–30.
49. Maruyama J, Maruyama K. Impaired nitric oxide-dependent responses and their recovery in hypertensive pulmonary arteries of rats. *Am J Physiol*. 1994;266:H2476–H2488.
50. Murata T, Sato K, Hori M, Ozaki H, Karaki H. Decreased endothelial nitric-oxide synthase (eNOS) activity resulting from abnormal interaction between eNOS and its regulatory proteins in hypoxia-induced pulmonary hypertension. *J Biol Chem*. 2002;277:44085–44092.
51. Shaul PW, Wells LB, Horning KM. Acute and prolonged hypoxia attenuate endothelial nitric oxide production in rat pulmonary arteries by different mechanisms. *J Cardiovasc Pharmacol*. 1993;22:819–827.
52. Lowson SM. Alternatives to nitric oxide. *Br Med Bull*. 2004;70:119–131.
53. Balakrishna S, Song W, Achanta S, Doran SF, Liu B, Kaelberer MM, Yu Z, Sui A, Cheung M, Leishman E, Eidam HS, Ye G, Willette RN, Thorneloe KS, Bradshaw HB, Matalon S, Jordt SE. TRPV4 inhibition counteracts edema and inflammation and improves pulmonary function and oxygen saturation in chemically induced acute lung injury. *Am J Physiol Lung Cell Mol Physiol*. 2014;307:L158–L172.
54. Thorneloe KS, Cheung M, Bao W, Alsaid H, Lenhard S, Jian MY, Costell M, Maniscalco-Hauk K, Krawiec JA, Olzinski A, Gordon E, Lozinskaya I, Elefante L, Qin P, Matasic DS, James C, Tunstead J, Donovan B, Kallal L, Waszkiewicz A, Vaidya K, Davenport EA, Larkin J, Burgert M, Casillas LN, Marquis RW, Ye G, Eidam HS, Goodman KB, Toomey JR, Roethke TJ, Jucker BM, Schnackenberg CG, Townsley MI, Lepore JJ, Willette RN. An orally active TRPV4 channel blocker prevents and resolves pulmonary edema induced by heart failure. *Sci Transl Med*. 2012;4:159ra148.
55. Villalta PC, Townsley MI. Transient receptor potential channels and regulation of lung endothelial permeability. *Pulm Circ*. 2013;3:802–815.
56. Sullivan MN, Gonzales AL, Pires PW, Bruhl A, Leo MD, Li W, Oulidi A, Boop FA, Feng Y, Jaggar JH, Welsh DG, Earley S. Localized TRPA1 channel $Ca^{2+}$ signals stimulated by reactive oxygen species promote cerebral artery dilation. *Sci Signal*. 2015;8:ra2.
57. Ju H, Zou R, Venema VJ, Venema RC. Direct interaction of endothelial nitric-oxide synthase and caveolin-1 inhibits synthase activity. *J Biol Chem*. 1997;272:18522–18525.
58. Straub AC, Lohman AW, Billaud M, Johnstone SR, Dwyer ST, Lee MY, Bortz PS, Best AK, Columbus L, Gaston B, Isakson BE. Endothelial cell expression of haemoglobin alpha regulates nitric oxide signalling. *Nature*. 2012;491:473–477.
59. Brook MM, Fineman JR, Bolinger AM, Wong AF, Heymann MA, Soifer SJ. Use of ATP-$MgCl_2$ in the evaluation and treatment of children with pulmonary hypertension secondary to congenital heart defects. *Circulation*. 1994;90:1287–1293.
60. Lyubchenko T, Woodward H, Veo KD, Burns N, Nijmeh H, Liubchenko GA, Stenmark KR, Gerasimovskaya EV. P2Y1 and P2Y13 purinergic receptors mediate $Ca^{2+}$ signaling and proliferative responses in pulmonary artery vasa vasorum endothelial cells. *Am J Physiol Cell Physiol*. 2011;300:C266–C275.
61. McMillan MR, Burnstock G, Haworth SG. Vasodilatation of intrapulmonary arteries to P2-receptor nucleotides in normal and pulmonary hypertensive newborn piglets. *Br J Pharmacol*. 1999;128:543–548.
62. Visovatti SH, Hyman MC, Goonewardena SN, Anyanwu AC, Kanthi Y, Robichaud P, Wang J, Petrovic-Djergovic D, Rattan R, Burant CF, Pinsky DJ. Purinergic dysregulation in pulmonary hypertension. *Am J Physiol Heart Circ Physiol*. 2016;311:H286–H298.
63. Yamamoto K, Sokabe T, Ohura N, Nakatsuka H, Kamiya A, Ando J. Endogenously released ATP mediates shear stress-induced $Ca^{2+}$ influx into pulmonary artery endothelial cells. *Am J Physiol Heart Circ Physiol*. 2003;285:H793–H803.
64. Rummery NM, Brock JA, Pakdeechote P, Ralevic V, Dunn WR. ATP is the predominant sympathetic neurotransmitter in rat mesenteric arteries at high pressure. *J Physiol*. 2007;582:745–754.
65. Yamamoto K, Furuya K, Nakamura M, Kobatake E, Sokabe M, Ando J. Visualization of flow-induced ATP release and triggering of $Ca^{2+}$ waves at caveolae in vascular endothelial cells. *J Cell Sci*. 2011;124:3477–3483.
66. Hill-Eubanks DC, Gonzales AL, Sonkusare SK, Nelson MT. Vascular TRP channels: performing under pressure and going with the flow. *Physiology (Bethesda)*. 2014;29:343–360.
67. Kohler R, Heyken WT, Heinau P, Schubert R, Si H, Kacik M, Busch C, Grgic I, Maier T, Hoyer J. Evidence for a functional role of endothelial transient receptor potential V4 in shear stress-induced vasodilatation. *Arterioscler Thromb Vasc Biol*. 2006;26:1495–1502.

68. Mendoza SA, Fang J, Gutterman DD, Wilcox DA, Bubolz AH, Li R, Suzuki M, Zhang DX. TRPV4-mediated endothelial $Ca^{2+}$ influx and vasodilation in response to shear stress. *Am J Physiol Heart Circ Physiol*. 2010;298:H466–H476.
69. Fan HC, Zhang X, McNaughton PA. Activation of the TRPV4 ion channel is enhanced by phosphorylation. *J Biol Chem*. 2009;284:27884–27891.
70. Denninger JW, Marletta MA. Guanylate cyclase and the NO/cGMP signaling pathway. *Biochim Biophys Acta*. 1999;1411:334–350.
71. Stasch JP, Pacher P, Evgenov OV. Soluble guanylate cyclase as an emerging therapeutic target in cardiopulmonary disease. *Circulation*. 2011;123:2263–2273.
72. Mercado J, Baylie R, Navedo MF, Yuan C, Scott JD, Nelson MT, Brayden JE, Santana LF. Local control of TRPV4 channels by AKAP150-targeted PKC in arterial smooth muscle. *J Gen Physiol*. 2014;143:559–575.
73. Giaid A, Saleh D. Reduced expression of endothelial nitric oxide synthase in the lungs of patients with pulmonary hypertension. *N Engl J Med*. 1995;333:214–221.
74. Goldenberg NM, Wang L, Ranke H, Liedtke W, Tabuchi A, Kuebler WM. TRPV4 is required for hypoxic pulmonary vasoconstriction. *Anesthesiology*. 2015;122:1338–1348.
75. Villalta PC, Rocic P, Townsley MI. Role of MMP2 and MMP9 in TRPV4-induced lung injury. *Am J Physiol Lung Cell Mol Physiol*. 2014;307:L652–L659.

# SUPPLEMENTAL MATERIAL

**Figure S1.** Specific TRPV4 channel agonists increase the number of sparklet sites per field of view in native ECs from fourth-order PAs.

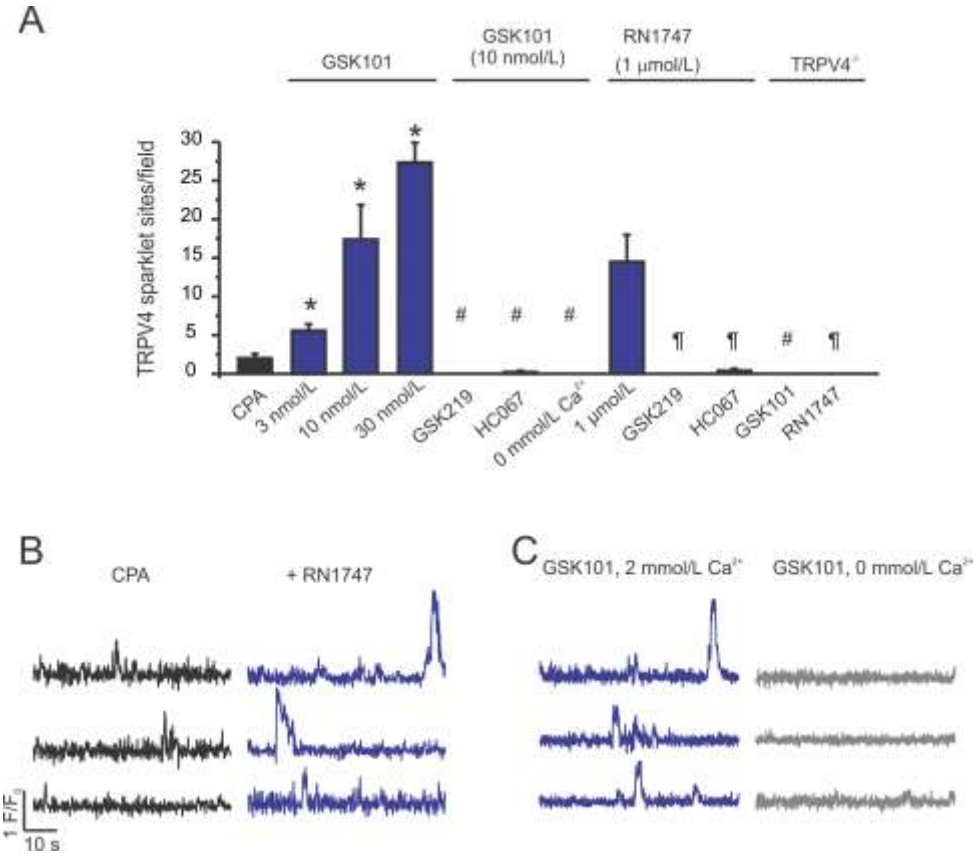


TRPV4 $Ca^{2+}$ sparklets were recorded in *en face* fourth-order PAs loaded with fluo-4AM (10 μmol/L). Cyclopiazonic acid (CPA, 20 μmol/L) was used in order to eliminate the interference from ER $Ca^{2+}$ release. A, Averaged number of TRPV4 sparklet sites per field under basal conditions (CPA), in the presence of TRPV4 agonist GSK101 (3-30 nmol/L), GSK101 (10 nmol/L) in the absence or presence of two different TRPV4 channel inhibitors (GSK219, 100 nmol/L and HC067047 or HC067, 1 μmol/L) or 0 mmol/L extracellular $Ca^{2+}$, another TRPV4 channel agonist RN1747 (1 μmol/L) in the absence or presence of TRPV4 inhibitors GSK219 (100 nmol/L) and HC067 (1 μmol/L), and GSK101 (10 nmol/L) and RN1747 (1 μmol/L) in the PAs from $TRPV4^{-/-}$ mice. Data are presented as mean ± SEM (n=5 PAs; $P<0.0001$ using one-way ANOVA; *, #, ¶ indicate significance ($P<0.05$) versus CPA, 10 nmol/L GSK101, and 1 μmol/L RN1747, respectively). B, Representative fractional fluorescence ($F/F_0$) traces of three distinct TRPV4 sparklet sites in a field of view in the absence (*left*) or presence (*right*) of the TRPV4 agonist RN1747 (1 μmol/L). C, Representative fractional fluorescence ($F/F_0$) traces of three distinct GSK1016790A (GSK101, 10 nmol/L)-induced TRPV4 sparklet sites in the presence (*left*) or absence (*right*) of extracellular $Ca^{2+}$ (2 mmol/L).

**Figure S2.** TRPV4 sparklets increase local, but not whole-cell $Ca^{2+}$ levels in the ECs.

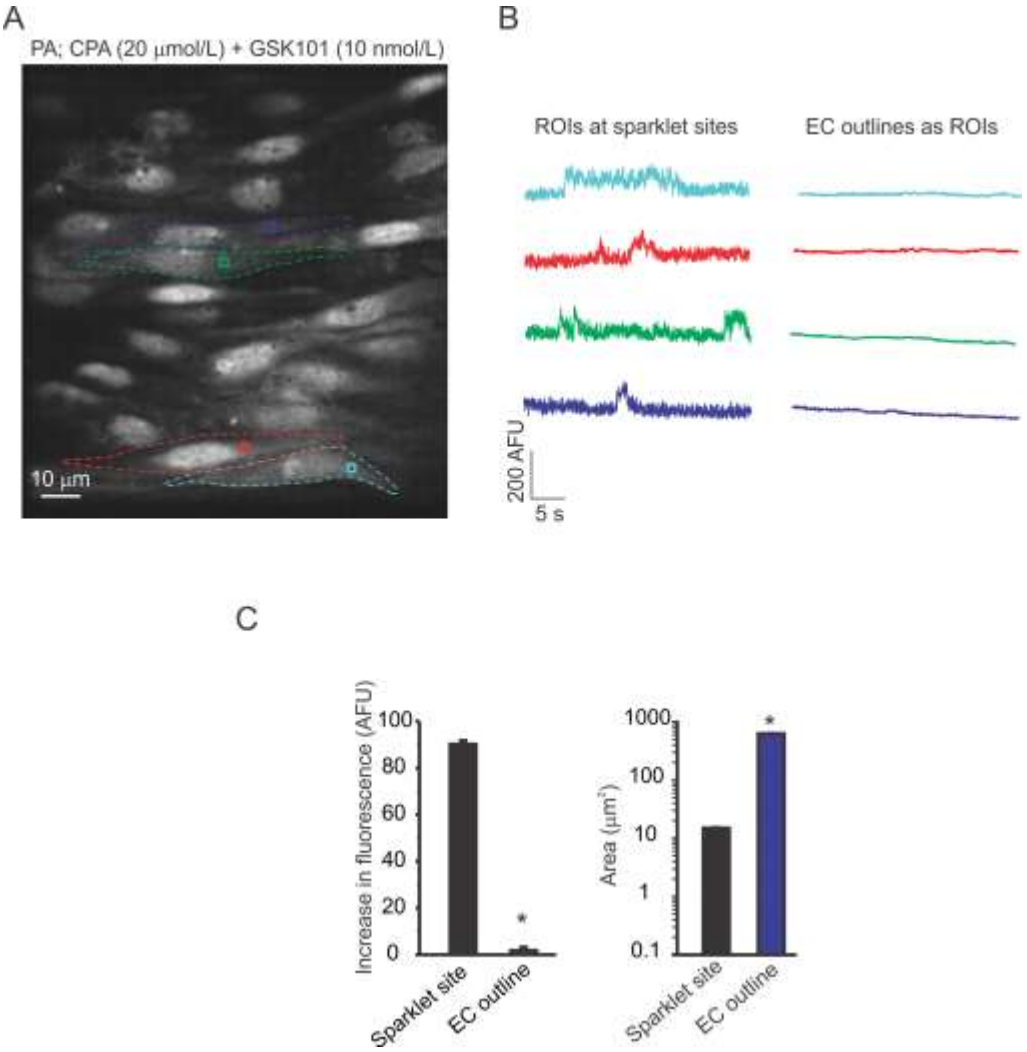


Changes in fluorescence were recorded in *en face* fourth-order PAs loaded with fluo-4AM (10 μmol/L) in the presence of GSK101 (10 nmol/L). Cyclopiazonic acid (CPA, 20 μmol/L) was used in order to eliminate the interference from $Ca^{2+}$ release from intracellular stores. A, A greyscale image of a field of view with ~ 15 ECs; the dotted lines indicates the outlines of ECs. Square boxes represent the regions of interest (ROIs) placed at the sparklet sites. B, Representative fluorescence traces of TRPV4 sparklets using square ROIs (*left*) and whole-cell fluorescence using whole-cell outlines as ROIs (*right*). C, Averaged increase in fluorescence (arbitrary fluorescence units; AFU) for ROIs placed at sparklet sites and whole cell ROIs following TRPV4 cannel activation with GSK101 (3 nmol/L; *left*); average spatial spread of sparklets and area encompassed by whole cell outlines (*right*). Data are presented as mean ± SEM (n=24 sparklet sites and 24 ECs; *P<0.0001 using independent t-test).

**Figure S3.** TRPV4 sparklets represent unitary $Ca^{2+}$ influx events through TRPV4 channels in the native endothelium from small PAs.

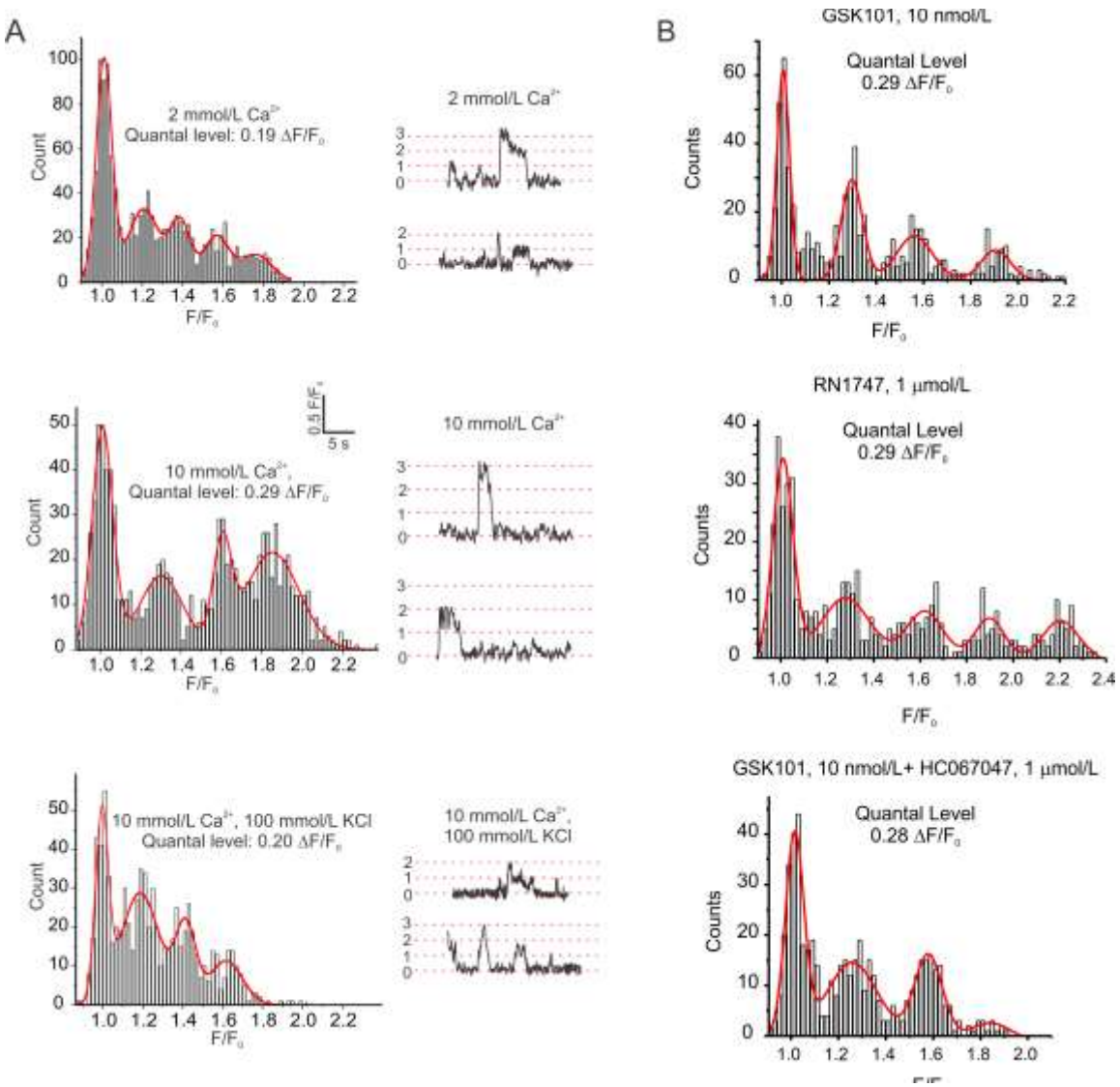


Localized $Ca^{2+}$ influx events through TRPV4 channels (TRPV4 sparklets) were recorded in *en face* fourth-order PAs from $GCaMP2^{Cx40}$ mice. Cyclopiazonic acid (CPA, 20 μmol/L) was used to eliminate the interference from $Ca^{2+}$ release from the endoplasmic reticulum (ER). Experiments were performed using 3 nmol/L GSK101 to increase the activity of TRPV4 sparklets in PAs from GCaMP2 mice. All-points histograms were constructed from the $F/F_0$ traces and were fit with a multiple Gaussian curve. The quantal levels (single-channel amplitudes) were derived from the peaks of the multiple Gaussian curve. The data were pooled from three PAs. Dotted lines represent the quantal levels (number of channels open) at a site. A, All-points histogram and representative traces in the presence of 2 mmol/L extracellular $Ca^{2+}$ (*top*) 10 mmol/L extracellular $Ca^{2+}$ (*middle*) and 10 mmol/L extracellular $Ca^{2+}$ and 100 mmol/L KCl (*bottom*). B, All-points histograms in the presence of a TRPV4 channel agonist GSK101 (10 nmol/L, *top*), a different TRPV4 channel agonist RN1747 (1 μmol/L, *middle*), and with the addition of a TRPV4 channel inhibitor HC067047 (1 μmol/L, *bottom*) in the presence of GSK101. The data were pooled from three PAs for each histogram.

**Figure S4.** Spermine NONOate, a NO donor, increases DAF-FM fluorescence in ECs and SMCs from small PAs and causes vasodilation in a concentration-dependent manner.

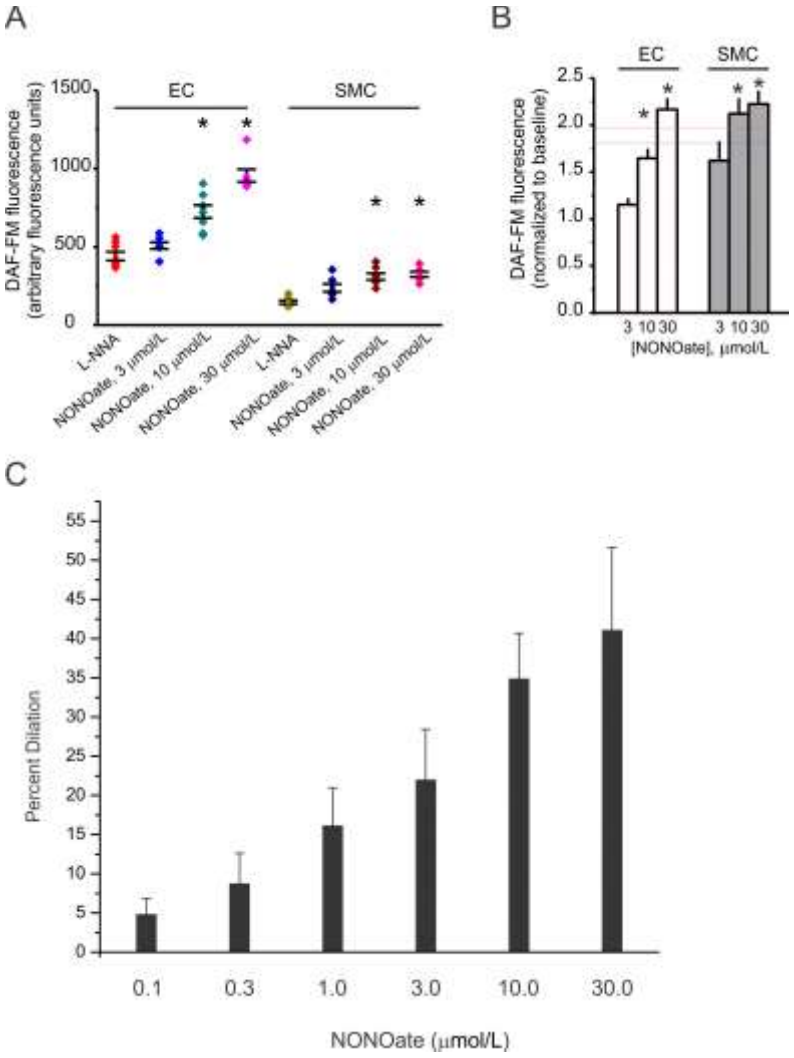


Nitric oxide (NO) fluorescence was recorded in *en face* fourth-order PAs using DAF-FM (fluorescent NO indicator; 5 μmol/L). The diameter studies were carried out in cannulated fourth-order PAs pressurized to 15 mmHg. A, Averaged DAF-FM fluorescence (arbitrary fluorescence units) in ECs and SMCs from PAs treated with L-NNA (100 μmol/L) alone and a combination of L-NNA and NONOate (3−30 μmol/L). Data are mean ± SEM; individual data points represent averaged fluorescence of all the ECs or SMCs in a field of view (n=8, 6, 8, 6, 6, 6, 7, 6 fields from left to right; P<0.0001 using one-way ANOVA; *P<0.05 versus L-NNA). B, Averaged NONOate-dependent change in DAF-FM fluorescence in ECs and SMCs from PAs relative to the fluorescence in the presence of L-NNA (baseline). Data are mean ± SEM (n=6, 8, 6, 6, 8, 6 fields from left to right; P<0.0001 using one-way ANOVA; *P<0.05 versus 3 μmol/L NONOate). The dotted blue line indicates GSK101-induced increase in DAF fluorescence in ECs, whereas dotted red line indicates GSK101-induced increase in DAF fluorescence in SMCs. C, Averaged percent dilations of PAs to NONOate (1-30 μmol/L; n=7, 9, 9, 9, 9, 6 PAs from left to right; P=0.0077 using one-way ANOVA).

**Figure S5.** $Ca^{2+}$ influx via endothelial TRPV4 channels does not increase $Ca^{2+}$ release from the endoplasmic reticulum (ER) in PAs.

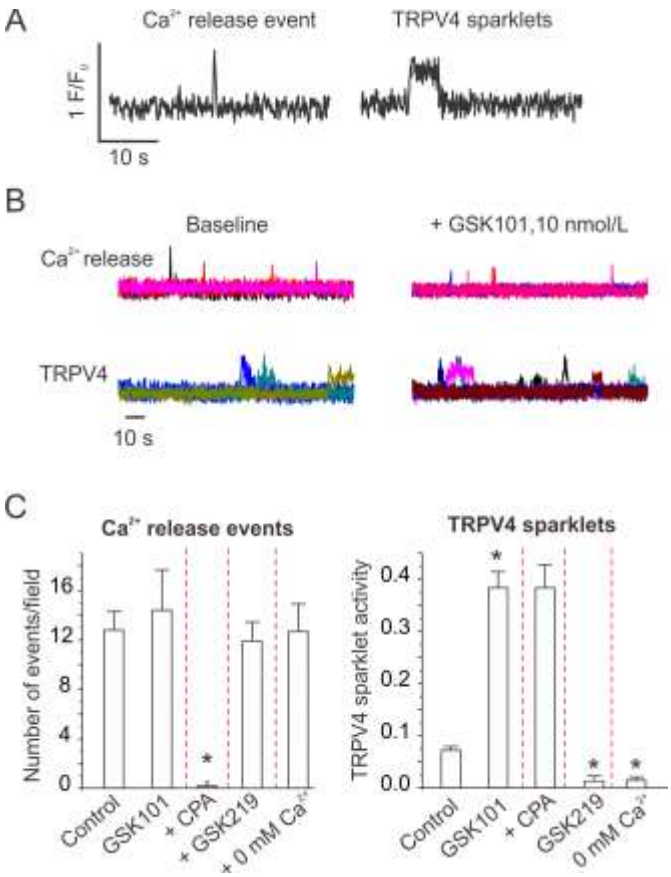


$Ca^{2+}$ events were simultaneously recorded in *en face* fourth-order PAs from GCaMP2$^{Cx40}$ mice. A, Representative fractional fluorescence ($F/F_0$) traces illustrating the differences in kinetics of $Ca^{2+}$ release from the ER (spike shape; less than 300 ms duration, *left*) and unitary $Ca^{2+}$ influx through TRPV4 channels ($Ca^{2+}$ sparklets; square event; greater than 300 ms duration, *right*). B, Representative $F/F_0$ traces of $Ca^{2+}$ pulsars (*top*) and $Ca^{2+}$ sparklets (*bottom*) under baseline condition and in the presence of GSK101 (10 nM). C, Averaged number of $Ca^{2+}$ pulsars per field in the absence (Control) and presence of GSK101 (10 nM), CPA (20 μM), TRPV4 inhibitor GSK219 (100 nM), and 0 mM extracellular $Ca^{2+}$ (*left*; n=5 fields; *P<0.05 versus control one-way ANOVA). Averaged $NP_O$ per field for TRPV4 sparklets (*right*; n=5 fields; *P<0.05 versus control one-way ANOVA) in the absence (Control) and presence of GSK101 (10 nM), CPA (20 μM), TRPV4 inhibitor GSK219 (100 nM), and 0 mM extracellular $Ca^{2+}$. Data are mean ± SEM; the TRPV4 sparklet activity is expressed as $NP_O$ where N represents the number of channels and $P_O$ is the open state probability of the channels).

**Figure S6.** Classical activators of endothelial $G_q$ protein-coupled receptors, carbachol (CCh) and bradykinin, do not increase EC TRPV4 $Ca^{2+}$ sparklet activity in small PAs.

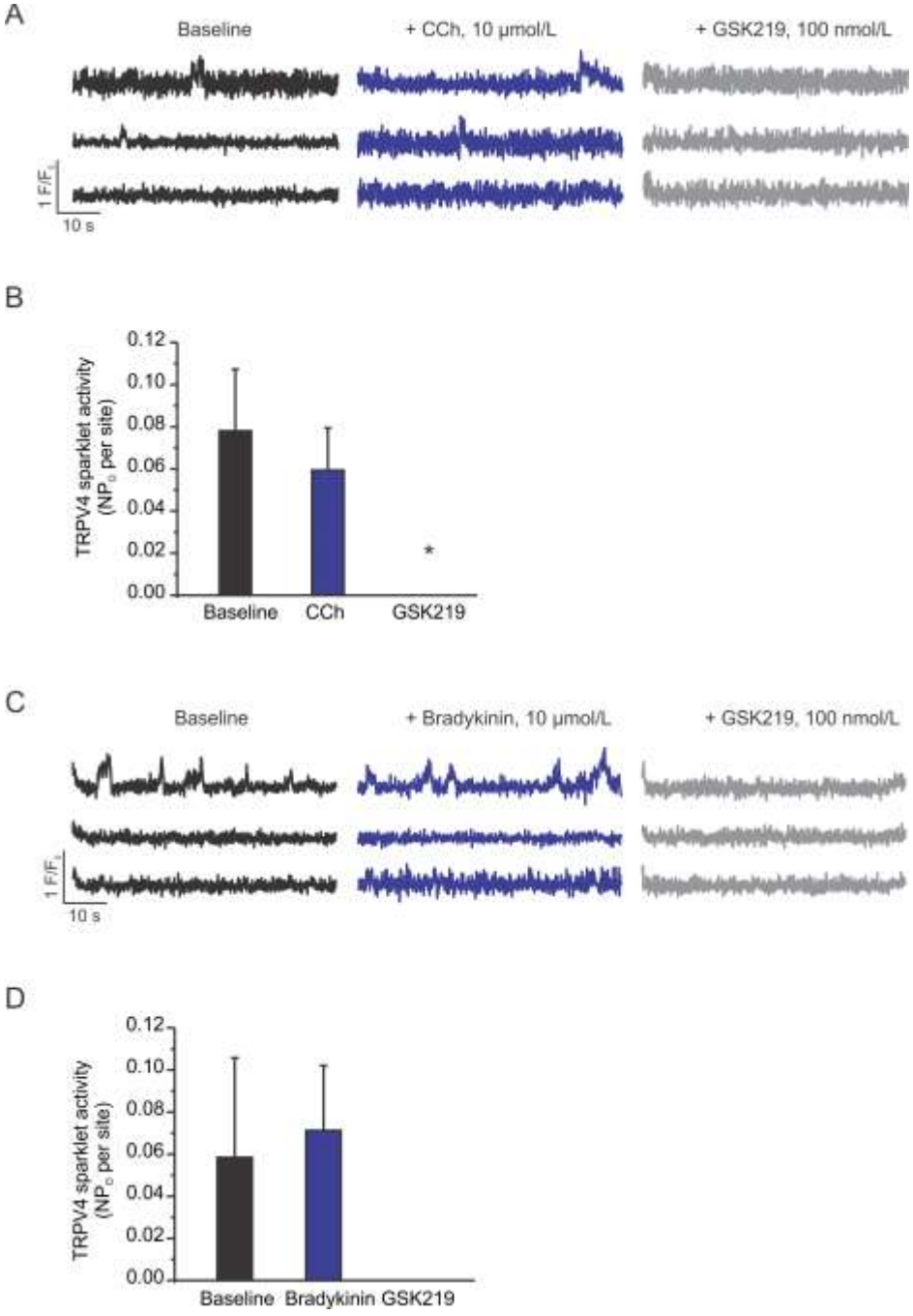


EC TRPV4 sparklet activity was examined in *en face* fourth-order PAs loaded with fluo-4AM (10 µmol/L) in the absence or presence of muscarinic (CCh) and bradykinin receptor (bradykinin)

activators. Cyclopiazonic acid (CPA, 20 μmol/L) was used throughout the $Ca^{2+}$ imaging experiments in order to eliminate the interference from $Ca^{2+}$ release from internal stores. A, Representative fractional fluorescence ($F/F_0$) traces of TRPV4 sparklets under baseline conditions (CPA, *left*), in the presence of the muscarinic receptor agonist (CCh, 10 μM, *middle*) and with the addition of TRPV4 inhibitor GSK219 (100 nmol/L, *right*). B, Averaged TRPV4 sparklet activity ($NP_O$ per site); data are mean ± SEM (n=4 fields; P=0.0105 using one-way ANOVA; *P<0.05 versus baseline). C, Three representative $F/F_0$ traces of TRPV4 sparklets under baseline conditions (CPA, *left*) or in the presence of bradykinin (10 μmol/L; *middle*), and with the addition of GSK219 (100 nmol/L; *right*). D, Averaged TRPV4 sparklet activity ($NP_O$ per site). Data are mean ± SEM (n=5, 8, 5 fields from left to right; P=0.1517 using one-way ANOVA).

**Video Legend:**

**Video S1.** TRPV4 sparklets in 4$^{th}$-order pulmonary arteries (PAs) in an *en face* preparation. PAs were loaded with fluo-4AM (10 μmol/L). Cyclopiazonic acid (CPA, 20 μmol/L) was used in order to eliminate the interference from ER $Ca^{2+}$ release. The activity of TRPV4 sparklets was increased using TRPV4 channel agonist GSK101 (3 nmol/L).